C.P. No. 83
12,666, 12,000
A.R.C. Technical Report

MINISTRY OF SUPPLY

AERONAUTICAL RESEARCH COUNCIL

CURRENT PAPERS

Wind Tunnel Tests on a 90° Apex Delta Wing of Variable Aspect Ratio (Sweepback 36·8°)

Part I. General Stability

by

J. G. Ross, B.Sc (Eng.), R. Hills, B.A.
and R. C. Lock, B.A.

Part II. Measurements of Downwash and Effect of High Lift Devices

by

R. C. Lock, B A., J. G Ross, B.Sc (Eng.),
and P. Meiklem

LONDON: HER MAJESTY'S STATIONERY OFFICE

1952

ELEVEN SHILLINGS NET.

C.P. No.83
(12,666, 12,000)
A.R.C. Technical Report

MINISTRY OF SUPPLY

AERONAUTICAL RESEARCH COUNCIL

CURRENT PAPERS

Wind Tunnel Tests on a 90° Apex Delta Wing of Variable Aspect Ratio (Sweepback 36.8°)

Part I. General Stability

by

J.G. Ross, B.Sc., R.Hills, B.A.
and
R.C. Lock, B.A.

Part II. Measurements of Downwash and Effect of High Lift Devices

by

R.C. Lock, B.A.,
J.G. Ross, B.Sc.(Eng.), A.F.R.Ae.S.,
and
P. Meiklem

C.P. No.83

Report No. Aero.2333

August, 1949

ROYAL AIRCRAFT ESTABLISHMENT

Wind Tunnel Tests on a 90° Apex Delta Wing of Variable Aspect Ratio (Sweepback 36.8°)

Part I - General Stability

by

J.G. Ross, B.Sc., R. Hills, B.A.
R.C. Lock, B.A.

SUMMARY

Longitudinal and lateral stability measurements have been made in a low speed tunnel on a delta wing of 90° apex angle with three different taper ratios. The tests included measurements with ground, the effect of a body, and measurements of elevon power.

C_{Lmax} was 0.86 for all taper ratios but was reduced to a trimmed value of 0.65 with a static margin of $0.10\bar{c}$, due to the large loss of lift caused by the elevons. A tip stall starts on the wings at $\alpha = 8°$ to 12° depending on the taper ratio; this has comparatively little effect on pitching moments but a large effect on both rolling and yawing moments, n_v and $-\ell_v$ both decreasing after the tip stall. C.A.T. tests suggest that there is an appreciable favourable scale effect on the tip stall. Ground effects are small and can be estimated sufficiently accurately using existing theoretical work on unswept wings.

LIST OF CONTENTS

LIST OF TABLES

LIST OF ILLUSTRATIONS

1 Introduction

A series of tunnel tests has been made on a wing of delta plan form to investigate its low speed characteristics. Some results have already been described briefly[1] in a preliminary note. This report discusses these in more detail* and in addition gives further results from some later investigations on the same model.

2 Description of model

The model consisted basically of a wing of triangular shape having an apex angle of 90° and aspect ratio 4. This gives an angle of sweep-back of 36.8° along the quarter chord line. The wing tips were removable in two stages so that aspect ratios of 3 and 2.31 could be obtained (Fig.1). In each case elevons were fitted which were of constant chord equal to 9.4% of the centre line chord C_1 of the wing. In the condition where the aspect ratio of the wing was 3, the rear portion of the wing containing the elevons was removable, and could be replaced by sections containing either of two sets of tapered elevons which were 20% or 15% of the local wing chord respectively. All elevon hinge gaps were kept sealed throughout. Relevant data are given in Table I. The wing was also tested in conjunction with a symmetrical body of circular cross section and a triangular shaped fin shown in Fig.1.

The tests were made in the R.A.E. No.2 $11\frac{1}{2}' \times 8\frac{1}{2}'$ tunnel during December 1946 and early 1947 at a tunnel speed of 200 ft/sec., giving Reynolds numbers of 2.7, 2.4, 2.1×10^6 based on the mean chords for the three aspect ratios. The tests included measurements of lift, drag and pitching moments with various elevon angles, some tests with a ground plate in the tunnel, and yawing and rolling moments due to sideslip and to elevons.

Further measurements of downwash behind the wing and of the effect of split flaps and nose flaps have been made and are reported in Ref.2.

Normal tunnel constraint corrections to incidence and drag have been applied to the tests without ground as for an unswept wing. With ground it was thought that the corrections would be very small and therefore none have been applied.

3 Discussion of results

3.1 Lift

The values of C_L for the three plan forms with zero elevon angles are plotted against incidence in Fig.2. A decrease in aspect ratio causes a slight decrease in lift curve slope, but has little effect on $C_{L_{max}}$. The value of 0.86 for $C_{L_{max}}$ is low, and tuft observations showed that a tip stall started at $\alpha = 8°$ to 12° depending on the aspect ratio. Fig.4 shows a typical set of surface tufts for the wing of aspect ratio 3. There was considerably less outflow than on a wing with a swept back trailing edge, so the early tip stall may be associated with the high local lift loading and low Reynolds number at the tips. In fact assuming a two dimensional $C_{L_{max}}$ of 0.8 for this wing section at low R and allowing for the theoretical lift distribution from Ref.3, the tip of the A = 3 wing would be expected to stall at an overall C_L of about 0.6 i.e. 10.5° incidence, in fair agreement with the tuft photographs in Fig.4.

---

* Revised strut corrections have been applied to the drag and pitching moment results and there are slight differences in the results given here as compared with Ref.1.

The body has little effect on $C_{L_{max}}$ or lift slope (Fig.3). Ground gives an appreciable increase in both, though the stall was not actually reached in the tests with ground (Fig. 2). The change in incidence due to ground at a given C_L is compared in Fig.5 with the estimated value from Ref.4 for a wing without sweepback. The agreement is good enough up to the region where the tip stall starts ($C_L \doteq 0.6$), and shows that this simple method of calculating ground effect is adequate for delta shapes.

3.2 Drag

The rapid rise in drag when the tip stalls is shown in Fig.6 where the effective profile drag (defined as $C_D - \frac{1}{\pi A} C_L^2$) is plotted against C_L. Some C.A.T. results[5] at high Reynolds number on a wing of the same plan form and section, also given in Fig.6, show that there is a considerable scale effect especially on the lowest aspect ratio wing. This would be expected if, as already suggested, the tip stall occurs at the two dimensional $C_{L_{max}}$ at the appropriate local Reynolds number. For the C.A.T. results at $R = 8 \times 10^6$ (mean) the local $C_{L_{max}}$ would be about 1.15 for the lowest aspect ratio wing corresponding to an overall mean $C_L = 0.96$ for the whole wing. For the R.A.E. tests at $R = 2.7 \times 10^6$ the local $C_{L_{max}} = 0.85$ and the corresponding mean $C_L = 0.7$.

Values of the induced drag factor K, defined by the equation,

$C_D = C_{D_0} + \frac{K}{\pi A} \cdot C_L^2$, are as follows at low lift coefficients:-

	A = 4	A = 3	A = 2.31
K	1.27	1.19	1.12

The C.A.T. tests[5] again show some favourable scale effect on these results.

Fig.7 shows the variation of gliding angle $\left(= \tan^{-1} \frac{C_D}{C_L}\right)$ with C_L for the wing of aspect ratio 3 at constant elevon angles. The broken curve indicates the gliding angle with elevons adjusted to trim, assuming a static margin of $0.10\bar{c}$ at low lift coefficients. It will be noticed that there is a rapid increase in gliding angle above a C_L of about 0.55, corresponding at a wing loading of 25 lb/sq.ft., to a speed of 130 m.p.h. Some appreciable scale effect may be expected as already mentioned.

3.3 Pitching moments

The pitching moment coefficients in the tables and in most of the figures are given about a C.G. at the same position (0.466 of centre line chord from apex) relative to the centre line chord for all aspect ratios. In Fig.8 however the moment curves are shown with C.G. positions adjusted to give the same static margin at zero C_L. These curves indicate the different behaviour of the wings at high lift coefficients. At the stall all the wings show a nose down pitching moment, but just before the stall the A = 4 wing becomes slightly unstable, while the A = 2.3 wing has a steadily increasing stability. This latter effect will make it difficult to stall the low aspect ratio wing since the pitching moment required for trimming is large.

The aerodynamic centres for the wings at low incidences are as follows, the calculated values being obtained by Falkner[3].

Table B

Wing Aspect Ratio A	Behind L.E. of centre line chord c_1	Behind L.E. of geometric mean chord $\bar{c}$	
	Measured	Measured	Calculated
2.31	$0.495\ c_1$	$0.29\ \bar{c}$	$0.273\ \bar{c}$
3	$0.534\ c_1$	$0.325\ \bar{c}$	$0.319\ \bar{c}$
4	$0.563\ c_1$	$0.375\ \bar{c}$	$0.383\ \bar{c}$

The effect of the body on pitching moments is small (Fig.9). Ground effect (Fig.10) is also fairly small and is compared in Fig.5 with the calculated effect[4] on a straight wing. Again the agreement is good enough for estimation.

3.4 Elevon effects on lift and pitching moments

From Figs.11 and 12 it appears that constant chord elevons are slightly more effective in producing a pitching moment change at a given lift coefficient than either of the tapered elevons. The loss of lift due to the elevons, which in all cases is large, is least for the 15% chord tapered ones and these elevons give the highest trimmed $C_{L_{max}}$ (0.65 with a static margin of $0.12\bar{c}$). To try and reduce the large lift loss due to the elevons, some tests were made with the inboard 25% span of the 20% chord tapered elevons cut off. The results given in Table VII showed that though the lift change is reduced, so also is the pitching moment and there is not sufficient elevator power to trim at high lift coefficients.

Cross plots of the elevon effect on lift and pitching moments at a given incidence (Fig.13) show clearly the effect of the tip stall in reducing the elevon power at high incidence. The effect is worst for the highest aspect ratio. Falkner has calculated the lift effectiveness of a 20% chord taper elevon on this wing* and by using a two dimensional value of 0.0095/degree for $\frac{dC_M}{d\eta}$, the overall pitching moment effect can be calculated. The following table shows reasonable agreement between the experimental and calculated values at zero incidence.

/Table

* The calculations were made for elevon spans of 100% and 90% of the wing span, the results have been extrapolated to the model elevon span of 86%.

Table C

Wing A = 3 20% chord elevons	Expt. with body	Calculated No body
$\frac{dC_L}{d\eta}$ /degree	0.023	0.0232
$\frac{dC_M}{d\eta}$ /degree	-0.0012	-0.00111

3.5 Yawing and rolling moments due to sideslip

The measurements with sideslip showed linear variation of yawing and rolling moments with angle of sideslip up to an incidence of about 10°, but at higher incidences when the wing tips stalled the curves became irregular (Fig.14). The value of the rolling and yawing moment at zero sideslip, plotted for a range of incidence in Fig.15, shows considerable asymmetry especially on rolling moments. This is presumably due to differences in the tip stall on the port and starboard sides of the wing. Though the asymmetry is well within the elevon power this sort of behaviour would obviously not be satisfactory on a full scale aircraft. As already indicated there should be a favourable scale effect on the tip stall so that lift coefficient available before this effect becomes marked should be higher at flight Reynolds numbers.

Values of ℓ_v and n_v for the various model conditions tested are shown in Figs.16 and 17; in the region where the C_n, β and C_ℓ, β curves are not linear, n_v and ℓ_v are mean values for $\beta = \pm 5°$. The number of incidences for which results are available is not sufficient to to define the curves exactly especially in the region of the largest values of $(-\ell_v)$ and n_v. Since the fall in n_v and $(-\ell_v)$ at a lift coefficient of just above 0.6 is due to the tip stall, there will in any case probably be an appreciable scale effect in this region and higher values of n_v and $(-\ell_v)$ may be obtained at flight values of Reynolds number.

The effects of body and fin on n_v are roughly independent of incidence. The body as might be expected has little effect on ℓ_v, while the fin reduces the change of ℓ_v with lift.

3.6 Elevon effects on rolling and yawing moments

The effect of one constant chord elevon on rolling and yawing moments on the various aspect ratio wings is shown in Fig.15. As with lift effects there is a falling off in the rolling power of the elevons at high incidence, particularly on the wing with the pointed tip. Fig.18 compares the effects of the 15% chord tapered elevons with those of constant chord. As would be expected the constant chord elevons have a greater rolling power, though the difference between the two is less at high incidences. There is an appreciably adverse yawing moment at high incidences especially for controls of this type used purely as ailerons and moved symmetrically from zero. For elevons moved equal amounts up and down from a trimmed up position it is smaller.

The 15% chord elevons are powerful enough to hold the wings level at $C_L = 0.6$ for up to 15° of sideslip using 10° of control on each side.

This C_L represents the largest value of $-\ell_v$ measured in the model tests and at higher or lower values of C_L the aileron angle required will be less. At flight Reynolds numbers, $-\ell_v$ might be somewhat higher at larger C_L, but the aileron power would also be increased at higher incidence, compensating for the higher $-\ell_v$.

REFERENCES

No.	Author	Title, etc.
1	Hills, Lock, Ross	Interim Note on wind tunnel tests on a delta wing. ARC 10,535 February, 1947.
2	Lock, Ross, Meiklan	Wind tunnel tests on a 90° apex delta wing of variable aspect ratio Part II Measurements of downwash and the effects of high lift devices. (See Part II of this Report).
3	Falkner	Calculated loadings due to incidence of a number of straight and swept back wings. R & M. 2596. June, 1948.
4	Fani, Faima, Simidu	The effect of ground on the aerodynamic characteristics of a monoplane wing. A.R.C.3376, September, 1937.
5	Jones, Miles, Pusey	Experiments in the compressed air tunnel on sweptback wings including two delta wings. A.R.C.11354, March, 1948.

TABLE I

Relevant Model Data

Wing

Thickness chord ratio - symmetrical			0.10
Angle of sweepback (L.E.)			45°
Centre-line chord c_1			3.2 ft.
Distance from nose of body to L.E. centre-line chord			0.98 ft.

	A = 4.0	A = 3.0	A = 2.31
Span b-ft.	6.4	5.485	4.685
Mean chord $\bar{c}$-ft.	1.6	1.818	2.028
Area S-ft^2	10.24	9.97	9.50
Taper ratio	0	0.14	0.25

Elevons

(a) Constant chord elevons

Chord (to hinge line)-ft.	0.3	0.3	0.3
Span (per elevon)-ft.	2.86	2.40	2.00
Area (per elevon)-ft^2	0.858	0.720	0.600

(b) 20% chord tapered elevons

Mean chord-ft.	0.321
Span (per elevon)-ft.	2.31
Area (per elevon)-ft^2	0.741

(c) 15% chord tapered elevons

Mean chord-ft.	0.241
Span (per elevon)-ft.	2.31
Area (per elevon)-ft^2	0.556

Fin

Mean chord ft.	1.043
Height above centre line body ft.	1.565
Area (to centre line of body)-ft^2	1.633
Fin arm (distance from $\frac{1}{2}$ centre line chord of wing to $\frac{1}{2}$ centre line chord of fin) ft.	1.55

C.G. position

On centre line chord	
Distance behind L.E. of centre line chord ft.	1.493
Distance behind L.E. in terms of c_1 (centre line chord)	0.466 c_1
Height of C.G. above ground ft.	0.834

Note

Note all C_M's are given about this C.G. except those in Fig.8. All values of C_n however are given about a C.G. at 0.366 ft. behind the above C.G. i.e. at 0.58 c_1 (c_1 = centre line chord).

TABLE II

Wing and Fin Ordinates

Distance from L.E. % chord	½ ordinate % chord
0	0
0.5	0.825
0.75	1.009
1.25	1.298
2.5	1.820
5.0	2.529
7.5	3.041
10	3.445
15	4.050
20	4.473
25	4.759
30	4.932
35	4.999
40	4.953
45	4.770
50	4.492
55	4.146
60	3.750
65	3.318
70	2.860
75	2.387
80	1.910
85	1.433
90	0.955
95	0.477
100	0

Body Ordinates

Distance from nose % length	Radius % length
0	0
2.61	2.838
5.22	3.933
10.43	5.374
15.65	6.333
20.87	7.023
26.09	7.471
31.30	7.732
36.52	7.826
41.74	7.764
46.96	7.565
52.17	7.252
56.96	6.855
61.74	6.365
66.52	5.797
71.30	5.155
76.09	4.445
80.87	3.662
85.65	2.807
90.43	1.888
95.22	0.939
100	0

TABLE III

No Ground

Wing Alone $\eta = 0^{\circ}$

α°	A = 2.31			A = 3			A = 4		
	C_L	C_D	C_m	C_L	C_D	C_m	C_L	C_D	C_m
- 4.1	-0.260	0.0149	0.020	-0.229	0.0144	0.020	-0.258	0.0146	0.051
- 2.0	-0.112	0.0091	-0.001						
0 1	-0.023	0.0068	0	-0.014	0.0069	-0.009	-0.019	0.0070	0.003
2.2	0.083	0.0074	-0.004	0.109	0.0081	-0.024			
4.3	0.191	0.0126	-0.010	0.226	0.0133	-0.037	0.234	0.0127	-0.045
6.3	0.285	0.0195	-0.015						
8.4	0.385	0.0295	-0.021	0.440	0.0324	-0.063	0.479	0.0337	-0.089
10.5	0.508	0.0456	-0.031						
12.6	0.619	0.0648	-0.042	0.688	0.0846	-0.098	0.680	0.0866	-0.115
14.6	0.729	0.1096	-0.059						
16.7	0.800	0.1799	-0.076	0.842	0.1962	-0.133	0.818	0.1955	-0.137
18.7	0.845	0.2424	-0.092	0.870	0.2543	-0.142			
20.7	0.860	0.2960	-0.106	0.880	0.3102	-0.156	0.868	0.3026	-0.171
22.7	0.852	0.3414	-0.122	0.861	0.3527	-0.165			
24.7	0.821	0.3751	-0.129				0.840	0.3837	
28.7	0.795	0.4310	-0.142				0.788	0.4359	-0.215

TABLE IV

No Ground Wing + Body

Constant Chord Elevons $\eta = 0^o$

α^o	A = 2.31			A = 3			A = 4		
	C_L	C_D	C_m	C_L	C_D	C_m	C_L	C_D	C_m
-4.1	-0.219	0.0178	0.011	-0.246	0.0177	0.030	-0.260	0.0170	0.056
0.1	-0.022	0.0091	0.002	-0.008	0.0091	0.004	-0.025	0.0089	0.009
2.2	0.092	0.0098	-0.003	0.094	0.0096	-0.010	0.105	0.0095	-0.018
4.3	0.187	0.0144	-0.006	0.216	0.0146	-0.022	0.230	0.0144	-0.041
6.3	0.286	0.0216	-0.009	0.322	0.0215	-0.033	0.347	0.0213	-0.060
8.4	0.403	0.0334	-0.017	0.452	0.0334	-0.050	0.462	0.0331	-0.079
10.5	0.498	0.0461	-0.023	0.565	0.0495	-0.068	0.577	0.0546	-0.096
12.6	0.620	0.0677	-0.035	0.671	0.0827	-0.079	0.669	0.0845	-0.104
14.6	0.730	0.1132	-0.051	0.744	0.1308	-0.086	0.745	0.1326	-0.110
16.7	0.788	0.1832	-0.070	0.796	0.1886	-0.096	0.801	0.1943	-0.124
18.7	0.828	0.2437	-0.077	0.835	0.2498	-0.108	0.835	0.4313	-0.135
20.7	0.852	0.2998	-0.087	0.861	0.3067	-0.119	0.861	0.3011	-0.149
22.7	0.853	0.3439	-0.096				0.857	0.3462	-0.155
24.7	0.841	0.3733	-0.120	0.803	0.3840	-0.149	0.806	0.3774	-0.177
28.7	0.805	0.4582	-0.130	0.801	0.4582	-0.165	0.803	0.4537	-0.201

TABLE V

No Ground Wing + Body

Constant Chord Elevons $\eta = -10^o$

α^o	A = 2.31			A = 3			A = 4		
	C_L	C_D	C_m	C_L	C_D	C_m	C_L	C_D	C_m
-0.1	-0.194	0.0164	0.085	-0.273	0.0177	0.130	-0.295	0.0185	0.169
4.1	-0.006	0.0096	0.081	-0.040	0.0096	0.101	-0.053	0.0097	0.124
8.2	0.195	0.0161	0.069	0.196	0.0154	0.072	0.200	0.0153	0.074
12.4	0.403	0.0352	0.052	0.443	0.0427	0.033	0.441	0.0403	0.026
16.5	0.627	0.1364	0.007	0.634	0.1407	-0.010	0.616	0.1327	-0.012
20.6	0.710	0.2488	-0.021	0.713	0.2534	-0.037	0.708	0.2496	-0.051

TABLE VI

Wing + Body

Tapered Elevons A = 3

20% Chord

α°	$\eta = 0^{\circ}$			$\eta = -5^{\circ}$			$\eta = -10^{\circ}$			$\eta = -15^{\circ}$		
	C_L	C_D	C_m	C_L	C_D	C_m	C_L	C_D	C_m	C_L	C_D	C_m
-4.1	-0.244	0.0168	0.026									
0.1	-0.015	0.0088	-0.001	-0.150	0.0113	0.063	-0.253	0.0179	0.118	-0.406	0.0297	0.182
2.2	0.099	0.0095	-0.014									
4.3	0.216	0.0143	-0.025	0.066	0.0093	0.039	-0.012	0.0099	0.090	-0.171	0.0145	0.156
6.3	0.323	0.0213	-0.039									
8.4	0.450	0.0333	-0.053	0.311	0.0211	0.009	0.217	0.0156	0.060	0.064	0.0133	0.124
12.6	0.674	0.0828	-0.082	0.556	0.0567	-0.028	0.454	0.0396	0.024	0.321	0.0280	0.083
16.7	0.817	0.1944	-0.111	0.733	0.1602	-0.066	0.665	0.1402	-0.023	0.539	0.1156	0.034
18.7	0.845	0.2543	-0.121	0.767	0.2221	-0.076	0.706	0.1963	-0.036	0.596	0.1766	0.015
20.7	0.865	0.3071	-0.128	0.793	0.2692	-0.084	0.743	0.2490	-0.049	0.644	0.2298	-0.002
22.7	0.848	0.3475	-0.134	0.799	0.3167	-0.095	0.758	0.2939	-0.060	0.662	0.2725	-0.013

TABLE VII

Wing + Body - No Ground A = 3

20% Chord Tapered Elevons (Inboard 7" Cut Off)

α^o	$\eta = -5^o$			$\eta = -10^o$			$\eta = -15^o$		
	C_L	C_D	C_m	C_L	C_D	C_m	C_L	C_D	C_m
0	-0.091	0.0101	0.038	-0.179	0.0139	0.082	-0.260	0.0212	0.125
4.1	0.270	0.0131	-0.012	0.049	0.0110	0.057	-0.025	0.0140	0.097
8.3	0.368	0.0259	-0.014	0.289	0.0206	0.026	0.216	0.0201	0.065
12.5	0.610	0.0684	-0.050	0.530	0.0499	-0.013	0.473	0.0474	0.022
16.6	0.767	0.1832	-0.086	0.711	0.1620	-0.057	0.657	0.1542	-0.027
18.6	0.799	0.2406	-0.096	0.752	0.2133	-0.071	0.710	0.2111	-0.046
20.7	0.826	0.2909	-0.105	0.790	0.2719	-0.082	0.746	0.2589	-0.059
22.7	0.821	0.3329	-0.114	0.796	0.3155	-0.091	0.757	0.3061	-0.068
24.6							0.715	0.3391	-0.088

TABLE VIII

Wing + Body - No Ground

15% Chord Tapered Elevons A = 3

α^o	$\eta = 0^o$			$\eta = -10^o$			$\eta = -15^o$		
	C_L	C_D	C_m	C_L	C_D	C_m	C_L	C_D	C_m
-3.9	-0.212	0.0153	0.024	-0.428	0.0322	0.131	-0.499	0.0406	0.164
-1.9	-0.093	0.0100	0.011	-0.326	0.0221	0.122	-0.404	0.0295	0.160
0.1	0.024	0.0086	-0.003	-0.220	0.0152	0.112	-0.302	0.0207	0.151
2.2	0.136	0.0104	-0.015	-0.098	0.0103	0.100	-0.176	0.0138	0.138
4.3	0.258	0.0167	-0.029	0.033	0.0100	0.082	-0.054	0.0109	-
6.4	0.361	0.0232	-0.041	0.140	0.0130	0.066	0.065	0.0119	0.104
8.5	0.480	0.0364	-0.057	0.264	0.0191	0.049	0.187	0.0159	0.087
12.7	0.691	0.0934	-0.083	0.509	0.0595	0.010	0.439	0.0483	0.043
16.8	0.813	0.2032	-0.099	0.658	0.1624	-0.015	0.593	0.1430	0.019
18.8	0.844	0.2628	-0.109	0.705	0.2211	-0.029	0.640	0.2020	0.008
20.8	0.865	0.3184	-0.122	0.730	0.2667	-0.043	0.677	0.2511	-0.015
22.8	0.835	0.3585	-0.133	0.730	0.3109	-0.059	0.677	0.2930	-0.033

TABLE IX

With Ground

Wing Alone $\eta = 0^{\circ}$

α°	A = 2.31			A = 3			A = 4		
	C_L	C_D	C_m	C_L	C_D	C_m	C_L	C_D	C_m
-4				-0.315	0.0144	0.043	-0.365	0.0151	0.078
-2				-0.170	0.0084	0.023	-0.202	0.0087	0.047
0	-0.035	0.0063	0.010	-0.028	0.0067	0.006	-0.058	0.0070	0.019
2				0.125	0.0081	-0.015	0.104	0.0075	-0.014
4	0.207	0.0120	-0.006	0.255	0.0130	-0.032	0.233	0.0115	-0.039
6				0.393	0.0205	-0.051	0.401	0.0195	-0.072
8	0.462	0.0304	-0.027	0.533	0.0307	-0.072	0.525	0.0309	-0.096
10	0.579	0.0425	-0.039	0.675	0.0490	-0.098	0.650	0.0518	-0.118
12	0.721	0.0704	-0.061	0.799	0.0953	-0.119	0.761	0.0948	-0.135
14	0.844	0.1484	-0.086	0.880	0.1581	-0.136	0.850	0.1559	-0.152
16	0.922	0.2143	-0.113	0.947	0.2283	-0.159			
18				1.000	0.2936	-0.182	0.989	0.2901	-0.207

TABLE X

With Ground Wing + Body $\eta = 0^{\circ}$

Constant Chord Elevons

α°	A = 2.31			A = 3			A = 4		
	C_L	C_D	C_m	C_L	C_D	C_m	C_L	C_D	C_m
0	-0.065	0.0082	0.017	-0.049	0.0081	0.020	-0.073	0.0080	0.027
4	0.182	0.0124	0.004	0.209	0.0123	-0.013	0.231	0.0122	-0.033
8	0.438	0.0294	-0.015	0.486	0.0279	-0.051	0.522	0.0308	-0.087
10	0.567	0.0422	-0.027	0.638	0.0462	-0.077	0.634	0.0478	-0.106
12	0.704	0.0641	-0.046	0.758	0.0858	-0.096	0.752	0.0892	-0.120
14	0.833	0.1394	-0.073	0.847	0.1551	-0.112	0.848	0.1559	-0.139
16	0.910	0.2123	-0.091	0.912	0.2205	-0.127	0.920	0.2252	-0.160

TABLE XI

With Ground Wing + Body $\eta = -10^{\circ}$

Constant Chord Elevons

α°	A = 3		
	C_L	C_D	C_m
0	-0.364	0.0179	0.160
4	-0.070	0.0096	0.122
8	0.220	0.0150	0.078
10	0.367	0.0229	0.054
12	0.522	0.0457	0.022
14	0.657	0.1078	-0.011
16	0.736	0.1736	-0.036

TABLE XII

With Ground Wing + Body A = 3

20% Chord Tapered Elevons

α^{o}	$\eta = 0^{o}$			$\eta = -5^{o}$			$\eta = -10^{o}$		
	C_L	C_D	C_m	C_L	C_D	C_m	C_L	C_D	C_m
-4	-0.328	0.0157		-0.501	0.0206	0.116	-0.639	0.0365	0.177
-2	-0.189	0.0108	0.030	-0.350	0.0156	0.100	-0.500	0.0252	0.163
0	-0.068	0.0080	0.019	-0.197	0.0100	0.084	-0.357	0.0165	0.152
2	0.093	0.0086	-0.001	-0.077	0.0079	0.071	-0.211	0.0111	0.135
4	0.223	0.0130	-0.017	0.091	0.0096	0.049	-0.078	0.0095	0.117
6	0.384	0.0209	-0.038	0.239	0.0144	0.026	0.093	0.0113	0.091
8	0.522	0.0307	-0.059	0.388	0.0220	0.004	0.224	0.0153	0.020
10	0.651	0.0454	-0.081	0.522	0.0336	-0.021	0.368	0.0229	0.046
12	0.780	0.0898	-0.104	0.643	0.0647	-0.041	0.533	0.0468	0.013
14	0.860	0.1583	-0.119	0.779	0.1391	-0.076	0.656	0.1046	-0.018
16	0.918	0.2192	-0.138	0.840	0.2052	-0.094	0.750	0.1786	-0.041
18	0.972	0.2857	-0.151	0.884	0.2557	-0.109	0.801	0.2297	-0.053

α^{o}	$\eta = -15^{o}$			$\eta = -20^{o}$			$\eta = -25^{o}$		
	C_L	C_D	C_m	C_L	C_D	C_m	C_L	C_D	C_m
0	-0.518	0.0281	0.205						
4	-0.225	0.0142	0.185						
8	0.086	0.0141	0.134	-0.022	0.0172	0.183	-0.087	0.0300	0.210
10	0.238	0.0191	0.107	0.126	0.0196	0.157	0.059	0.0291	0.184
12	0.396	0.0419	0.074	0.276	0.0264	0.128	0.203	0.0322	0.156
14	0.539	0.0850	0.040	0.434	0.0661	0.093	0.352	0.0536	0.124
16	0.633	0.1506	-0.014	0.535	0.1349	0.066	0.441	0.1254	0.101

TABLE XIII

Yawing Moment Coefficients with Sideslip

Wing Alone $\eta = 0^{\circ}$

α	C_L	$10^3\ C_n$									N_v
		β=15	10	5	2	0	-2	-5	-10	-15	
A = 2.31											
0.1	-0.02	-	-	0.2	-	-0.7	-	-0.5	-	-	0.003
8.4	0.38	-	3.1	1.5	-	-0.6	-	-1.6	-3.4	-	0.018
12.6	0.62	7.1	4.5	2.0	0.9	0.8	-0.1	-1.6	-4.4	-7.2	0.021
A = 3											
0.1	-0.01	0.3	0.6	0	-0.4	-0.5	-0.5	-0.4	-1.2	-0.6	0.002
8.4	0.44	-	2.3	1.1	-	-0.5	-	-1.1	-2.8	-	0.013
12.6	0.69	6.4	4.1	1.9	-0.1	-0.6	-1.0	-2.1	-5.0	-7.2	0.023
16.7	0.84	9.3	5.5	1.5	0.4	0.2	0.1	-1.2	-4.8	-7.6	0.016
20.7	0.88	-4.1	-3.8	-2.0	-0.4	0.5	2.1	4.2	3.1	3.2	-0.035
A = 4											
0.1	-0.02	-	-	0	-	-0.5	-	-0.4	-	-	0.002
8.4	0.48	-	1.9	0.8	-	-0.6	-	-0.8	-2.0	-	0.009
12.6	0.68	6.7	4.8	2.1	-	-0.8	-	-2.3	-4.7	-6.8	0.025
16.7	0.82	7.6	4.9	1.4	0.2	-0.5	-0.9	-1.1	-4.3	-6.6	0.014

Rolling Moment Coefficients with Sideslip

Wing Alone $\eta = 0^{\circ}$

α	C_L	$10^3\ C_\ell$									ℓ_v
		β=15	10	5	2	0	-2	-5	-10	-15	
A = 2.31											
0.1	-0.02	-	-	0	-	0	-	0	-	-	0
8.4	0.38	-	-16.8	-9.2	-	-1.6	-	6.9	14.7	-	-0.093
12.6	0.62	-29.8	-21.8	-11.8	-6.4	-3.4	1.2	7.8	18.4	28.5	-0.117
A = 3											
0.1	-0.01	0	-0.6	-0.9	-1.2	-1.1	-1.0	-0.7	-0.4	-0.5	-0.002
8.4	0.44	-	-13.2	-7.3	-	-1.1	-	5.7	12.1	-	-0.075
12.6	0.69	-24.0	-16.8	-8.6	-4.6	-1.5	1.4	5.9	15.4	24.2	-0.084
16.7	0.84	-13.2	-8.3	-6.9	-7.1	-6.8	-4.8	2.2	4.8	8.5	-0.052
20.7	0.88	12.6	3.7	-1.8	-4.1	-3.1	-4.2	-5.8	-3.5	-6.4	0.023
A = 4											
0.1	-0.02	-	-	-1.6	-	-0.9	-	-2.7	-	-	0.007
8.4	0.48	-	-11.6	-6.3	-	-0.6	-	4.9	10.9	-	-0.064
12.6	0.68	-16.7	-11.9	-5.8	-	-0.8	-	4.3	11.5	18.3	-0.058
16.7	0.82	-8.3	-6.2	-2.7	-2.2	-0.5	2.5	3.1	3.2	6.3	-0.034

TABLE XIV

Yawing Moment, Rolling Moment and Sideforce Coefficients with Sideslip

Wing, Body and Fin $A = 3$ $\eta = 0°$

α	C_L	$\beta = 10°$	$5°$	$2.5°$	0	$-2.5°$	$-5°$	$-10°$	N_v
$10^3 C_n$									
0	0.004	12.3	5.7	2.9	0.3	-2.2	-4.7	-11.3	0.060
8.3	0.450	15.5	7.2	2.9	0.4	-3.0	-6.5	-14.9	0.078
12.5	0.672	18.2	8.8	4.8	0.4	-3.8	-8.2	-17.5	0.097
16.6	0.812	17.5	8.4	4.2	0.3	-3.9	-7.7	-16.9	0.092
20.6	0.843	4.9	4.4	2.4	0.3	-2.1	-3.6	- 6.1	0.046
$10^3 C_\ell$									ℓ_v
0	0.004	- 6.8	- 3.2	- 0.9	0.7	2.3	3.8	7.6	-0.040
8.3	0.450	-16.3	- 8.1	- 3.9	0.1	4.2	8.3	17.3	-0.094
12.5	0.672	-15.8	- 7.7	- 2.8	0.5	4.7	8.7	17.7	-0.094
16.6	0.812	-10.9	- 6.1	- 3.7	1.0	5.1	7.3	11.1	-0.077
20.6	0.843	- 5.5	- 1.1	0.7	-0.2	-1.1	0.7	5.2	-0.010
$10^3 C_y$									Y_v
0	0.004	-82.2	-39.1	-18.9	3.7	19.3	38.7	79.7	-0.23
8.3	0.450	-89.2	-43.2	-19.5	-0.2	21.4	41.4	87.1	-0.25
12.5	0.672	-95.7	-47.9	-22.7	-4.6	22.1	45.2	91.6	-0.27
16.6	0.812	-101.0	-49.3	-23.8	-2.7	22.5	47.6	102.0	-0.28
20.6	0.843	-82.5	-50.0	-25.4	-2.5	23.6	46.9	85.4	-0.27

Wing + Body $A = 3$ $\eta = 0°$

α	C_L	$\beta = 10°$	$5°$	$2.5°$	0	$-2.5°$	$-5°$	$-10°$	N_v
$10^3 C_n$									
0	0.005	- 6.0	- 3.1	-1.5	0.1	1.9	3.4	6.2	-0.037
8.3	0.461	- 4.7	- 2.4	-1.0	0.2	1.4	2.6	4.3	-0.029
12.5	0.726	- 2.7	- 0.8	-0.4	0.9	1.8	2.4	2.6	-0.018
16.6	0.839	- 5.0	- 3.2	-0.6	0	1.4	3.0	5.4	-0.035
20.6	0.832	-10.1	- 7.6	-4.1	0.8	6.0	9.2	10.9	-0.097
$10^3 C_\ell$									ℓ_v
0	0.005	0	0.4	0.2	0.4	-0.6	0.3	2.2	0.0005
8.3	0.461	-13.6	- 6.6	-3.5	0.2	4.0	8.0	15.0	-0.084
12.5	0.726	-10.4	- 4.9	-0.4	2.9	3.4	8.9	13.6	-0.079
16.6	0.839	- 7.7	- 5.1	-5.4	0.3	5.1	7.1	9.7	-0.070
20.6	0.832	- 1.3	4.3	3.7	1.0	-2.5	-2.0	4.0	+0.036
$10^3 C_y$									Y_v
0	0.005	- 6.5	- 2.3	-1.0	0.4	1.6	3.3	8.1	-0.02
8.3	0.461	- 9.4	- 3.9	-2.3	-1.0	1.1	3.7	9.0	-0.025
12.5	0.726	-12.5	- 5.3	-3.8	-3.1	-0.6	2.2	10.1	-0.03
16.6	0.839	-17.6	- 2.0	-0.3	-3.7	+0.3	4.4	14.6	-0.02
20.6	0.832	-31.0	-13.6	-7.2	-6.4	4.1	8.3	25.5	-0.07

TABLE XV

Effect of Elevons on Rolling and Yawing Moments

Constant Chord Elevon - Port Side Only Moved η + ve Trailing Edge Down

$\beta = 0^o$

Yawing Moment Coefficients $10^3\ C_n$

α	Wing Alone						Wing + Body	
	A = 2.31		A = 3		A = 4		A = 2.31	
	$\eta=0^o$	$\eta=+10^o$	$\eta=0^o$	$\eta=+10^o$	$\eta=0^o$	$\eta=+10^o$	$\eta=0^o$	$\eta=+10^o$
0.1	-0.9	-0.8	-0.4	-0.7	-0.3	-1.1	0.1	-0.8
4.3	-	-	-0.5	-	-	-	0.2	-2.0
8.4	-0.6	-3.4	-0.4	-3.4	-0.5	-4.6	0.1	-3.4
12.6	0.8	-4.4	-0.3	-4.8	-0.7	-5.5	1.5	-4.6
14.6	-0.6	-5.0	-	-4.9	-0.3	-4.8	0.4	-4.6
16.7	-0.8	-5.2	0.3	-4.9	-0.4	-4.6	0.3	-5.6
18.7	0.1	-5.5	0.6	-	0.1	-4.6	1.1	-5.3
20.7	0.4	-5.8	0.6	-4.6	0.2	-4.9	1.8	-5.6
22.7	2.5	-5.1	-	-0.5	1.3	-4.8	-	-7.2

Rolling Moment Coefficients $10^3\ C_\ell$

α	Wing Alone						Wing + Body	
	A = 2.31		A = 3		A = 4		A = 2.31	
	$\eta=0^o$	$\eta=+10^o$	$\eta=0^o$	$\eta=+10^o$	$\eta=0^o$	$\eta=+10^o$	$\eta=0^o$	$\eta=+10^o$
0.1	-1.0	18.3	-1.3	21.3	-1.1	23.6	-0.5	21.0
4.3	-	-	-1.3	-	-	-	-0.8	20.8
8.4	-1.6	17.7	-1.2	20.9	-0.9	15.8	-1.2	20.4
12.6	-3.3	16.8	-1.7	14.0	-1.6	10.9	-2.8	19.6
14.6	-2.0	16.4	-	9.0	2.5	9.7	-1.0	20.2
16.7	-4.1	10.4	-7.5	7.5	0	8.6	-3.0	13.5
18.7	-2.5	11.0	-5.0	-	-0.6	9.4	-4.0	11.5
20.7	-2.2	10.9	-3.2	8.7	-0.7	9.6	-4.2	10.9
22.7	-4.6	9.8	-	8.8	-2.4	8.5	-	11.3

TABLE XV (Cont'd.)

Wing + Body A = 3

Constant Chord Elevons - Port Side Only Moved (η + ve T.E. Down)

$\beta = 0^\circ$

α	$10^3\ C_\ell$				$10^3\ C_n$			
	$\eta=+10^\circ$	$\eta=0^\circ$	$\eta=-10^\circ$	$\eta=-20^\circ$	$\eta=+10^\circ$	$\eta=0^\circ$	$\eta=-10^\circ$	$\eta=-20^\circ$
0	22.8	-0.3	-22.9	-42.7	-0.6	0.1	-0.6	-3.0
4.2	22.8	-0.2	-22.5	-43.2	-1.8	0	0.4	-1.1
8.4	22.8	-0.3	-23.0	-42.0	-3.6	0 2	1.4	0.8
12.5	16.1	-1.9	-20.3	-36.1	-5.0	1.2	4.7	6.4
14.5	14.7	-0.5	-16.3	-34.8	-4.4	0.2	5.5	7.5
16.6	10.9	-0.5	-12.9	-29.6	-4.8	0.4	5.3	6.8
18.6	11.0	-1.5	-13.0	-24.7	-4.8	0.8	5.0	7.9
20.6	8.6	-1.2	-14.5	-29.4	-4.1	1.5	6.0	9.0
22.5		-7.6	-13.3	-31.9		5.7	9.5	10.7

15% Chord Tapered Elevons - Port Side Only Moved (η- ve up)

$\beta = 0^\circ$

α	$10^3\ C_\ell$				$10^3\ C_n$			
	$\eta=+10^\circ$	$\eta=0^\circ$	$\eta=-10^\circ$	$\eta=-20^\circ$	$\eta=+10^\circ$	$\eta=0^\circ$	$\eta=-10^\circ$	$\eta=-20^\circ$
0	19.7	0.6	-18.6	-32.4	-0.6	0.3	-0.1	-1.9
4.2	19.3	0.6	-18.7	-31.8	-1.7	0.1	0.6	-0.2
8.4	16.9	0.1	-19.0	-32.9	-2.9	0.3	1.8	1.4
12.5	15.4	1.4	-15.6	-27.8	-3.6	0.7	3.6	0.8
14.5	14.0	1.5	-11.5	-24.5	-3.6	0.6	4.8	6.2
16.6	11.0	1.5	-10.1	-20.6	-3.7	0.5	4.2	6.1
18.6	5.2	0.8	-10.8	-20.6	-3.4	0.1	3.8	6.4
20.6	7.1	-0.5	-11.5	-21.5	-2.9	0.4	4.4	6.9
22.5	3.3	-1.9	-12.0	-23.5	-1.2	1.5	4.9	7.1

FIG. 1

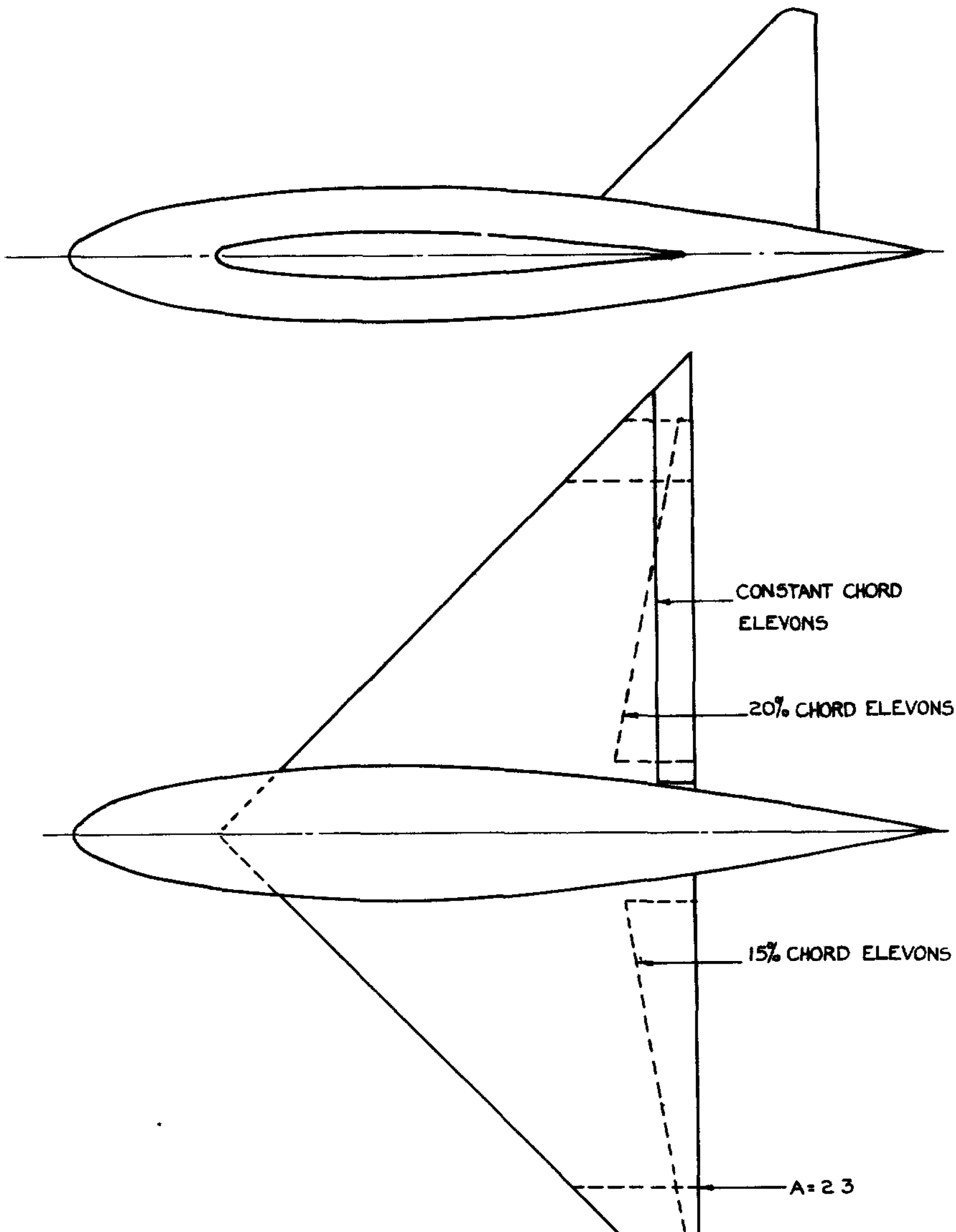

PLAN OF MODEL.

FIG. 2

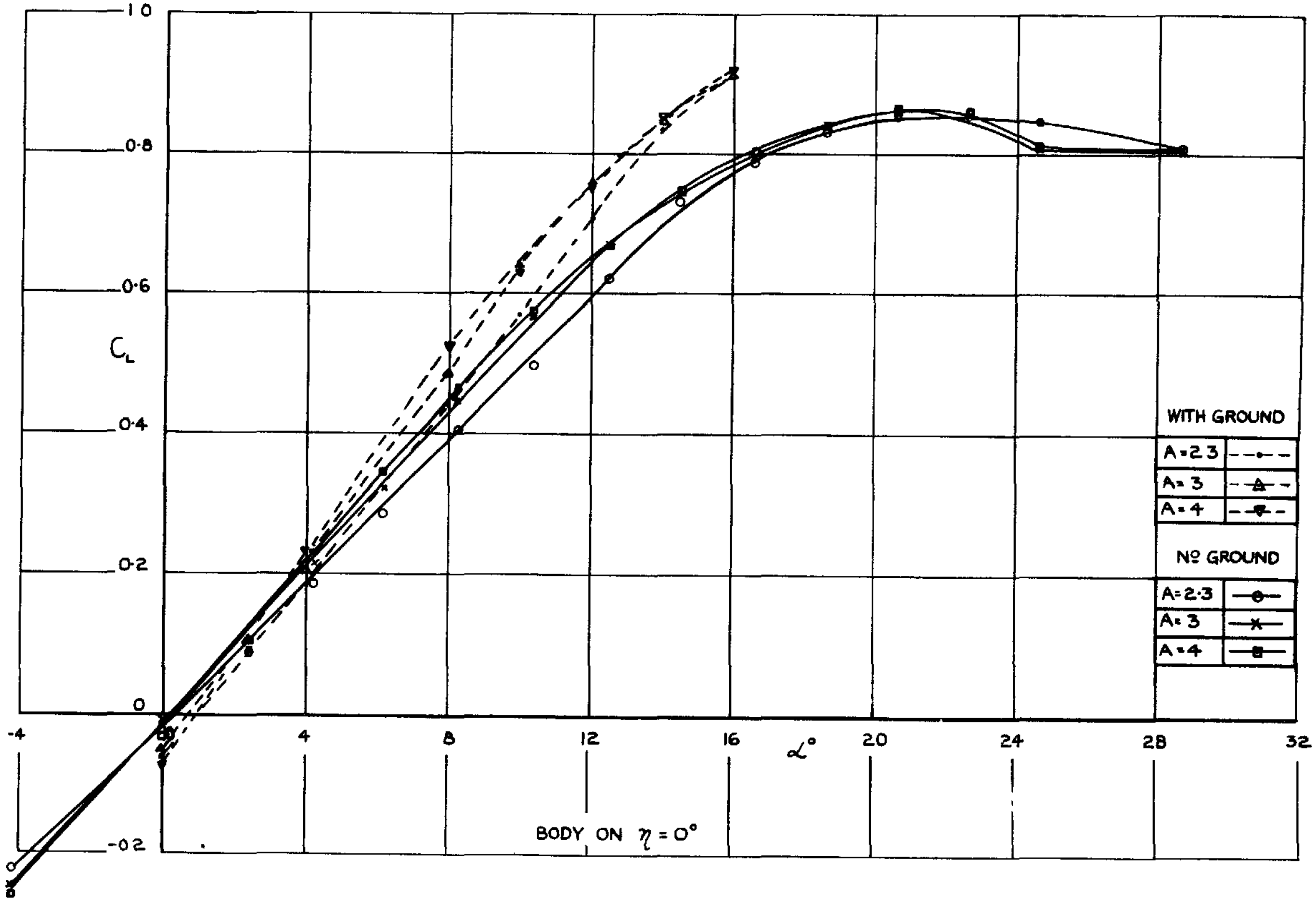

LIFT ON WINGS OF VARIOUS ASPECT RATIOS.

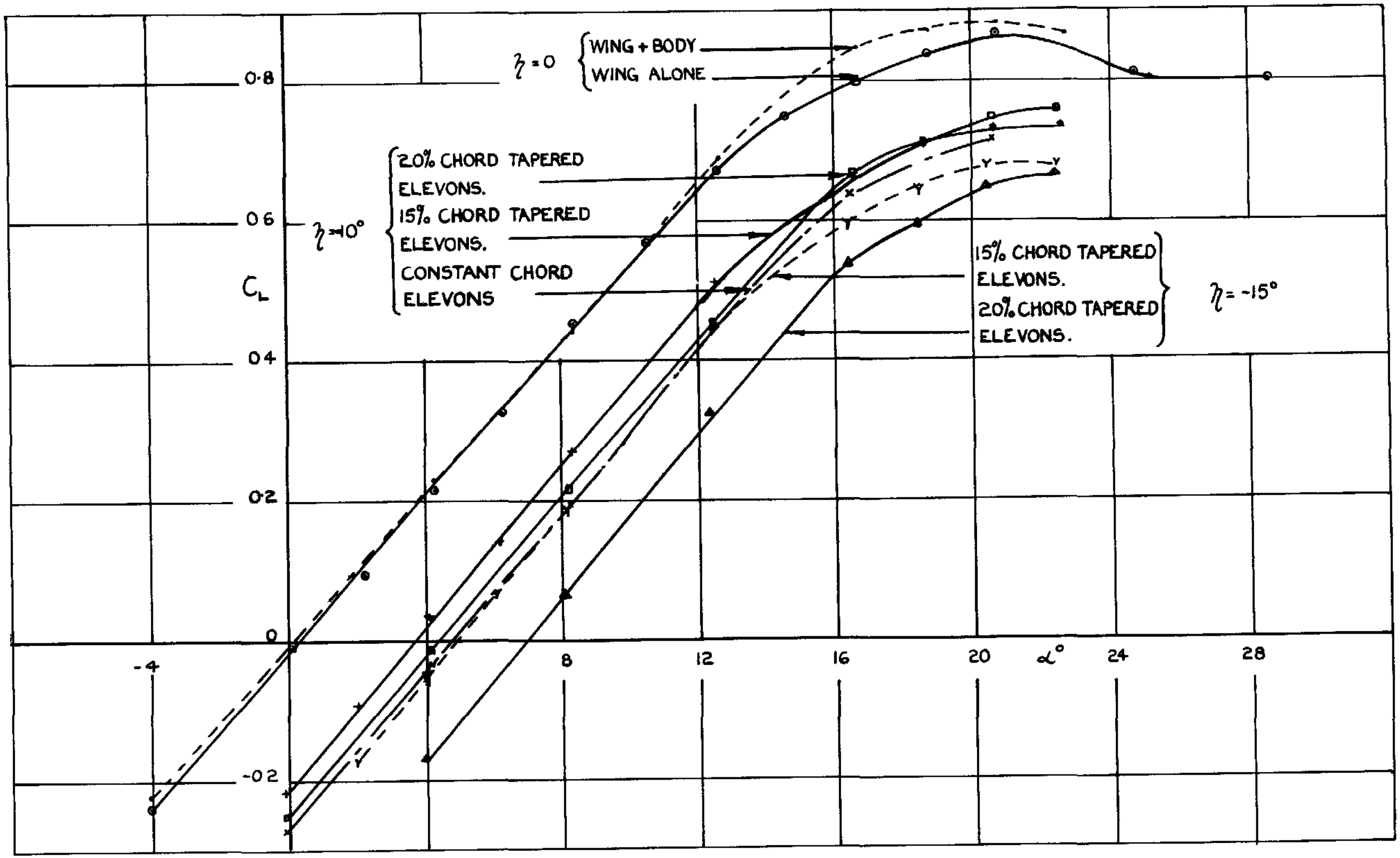

A= 3 WING WITHOUT GROUND.

EFFECT OF ELEVONS AND BODY ON LIFT.

FIG.3

FIG. 5

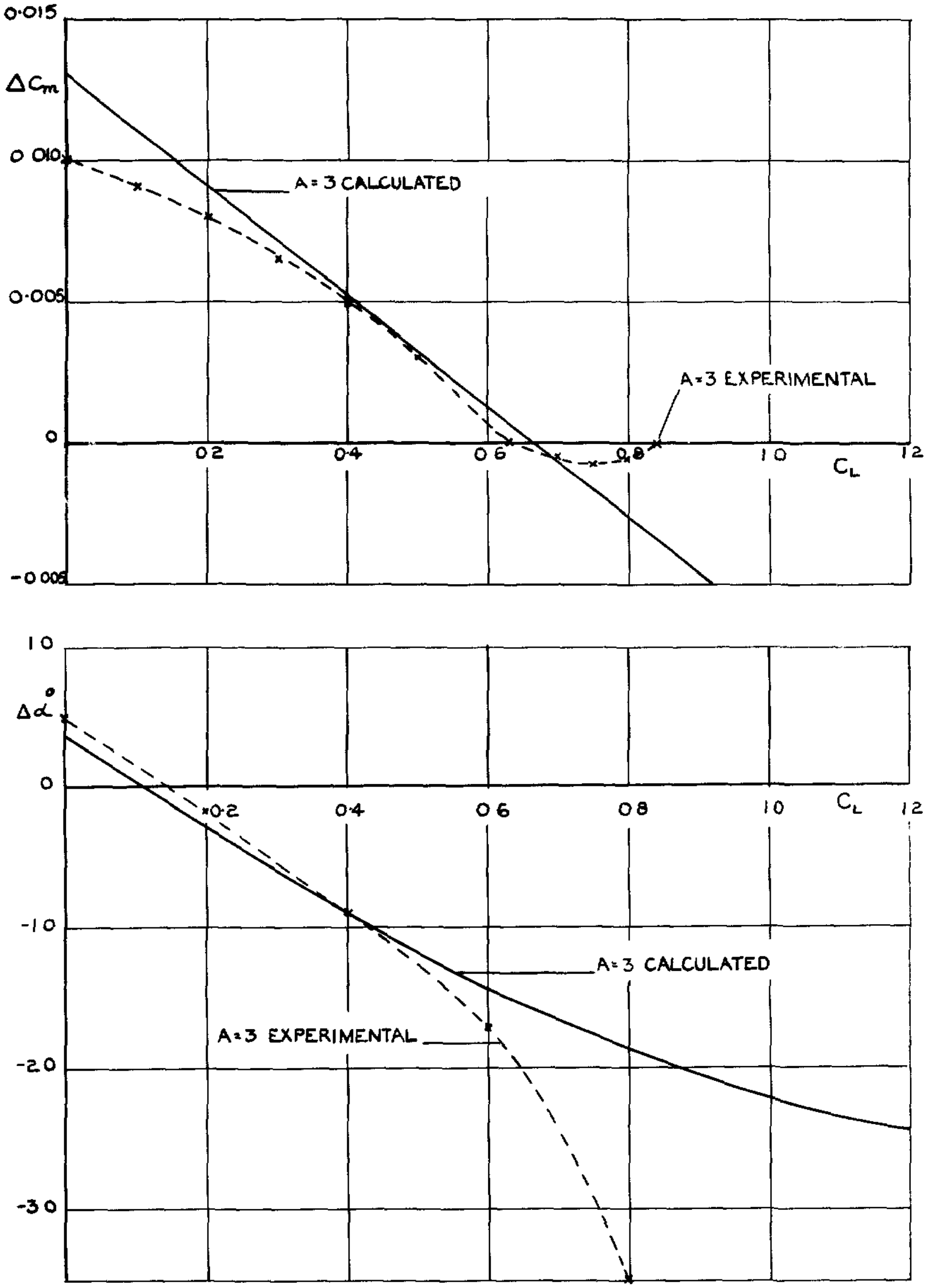

EFFECT OF GROUND ON LIFT AND PITCHING MOMENTS.

FIG. 6.

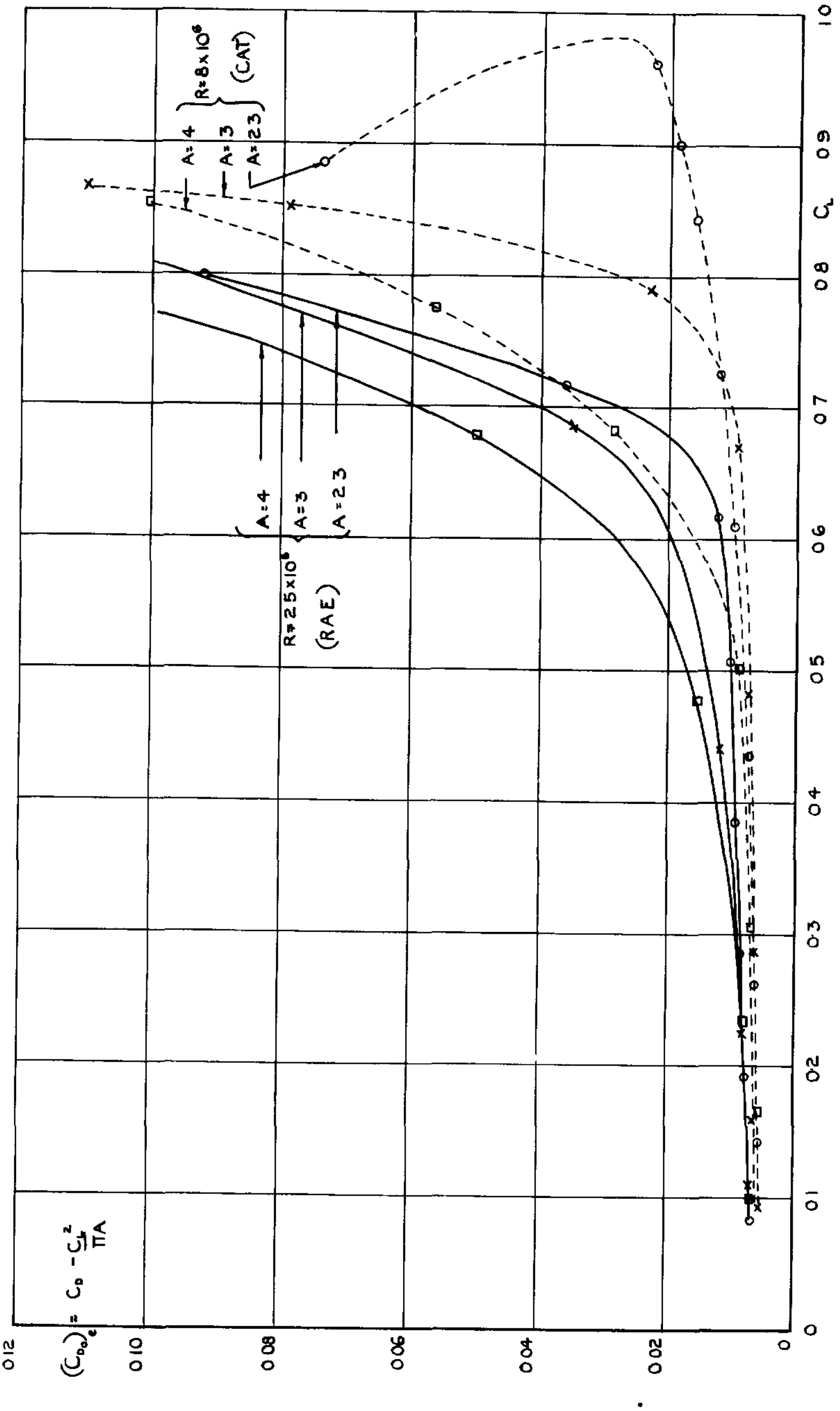

EFFECTIVE PROFILE DRAG.
(WING ALONE)

FIG. 7.

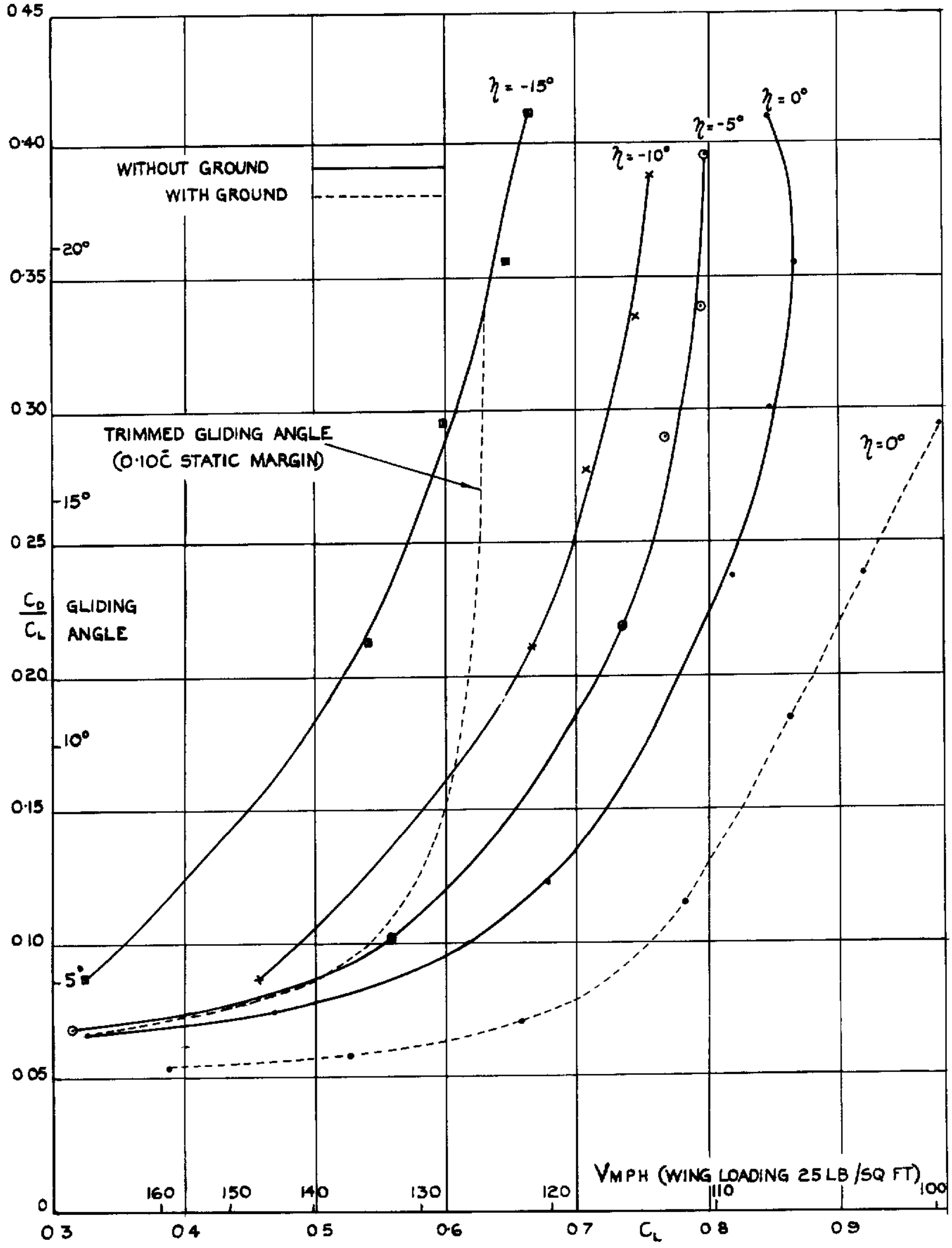

20% CHORD TAPERED ELEVONS

WING + BODY A = 3 WITH AND WITHOUT GROUND

ANGLE OF GLIDE.

FIG. 8.

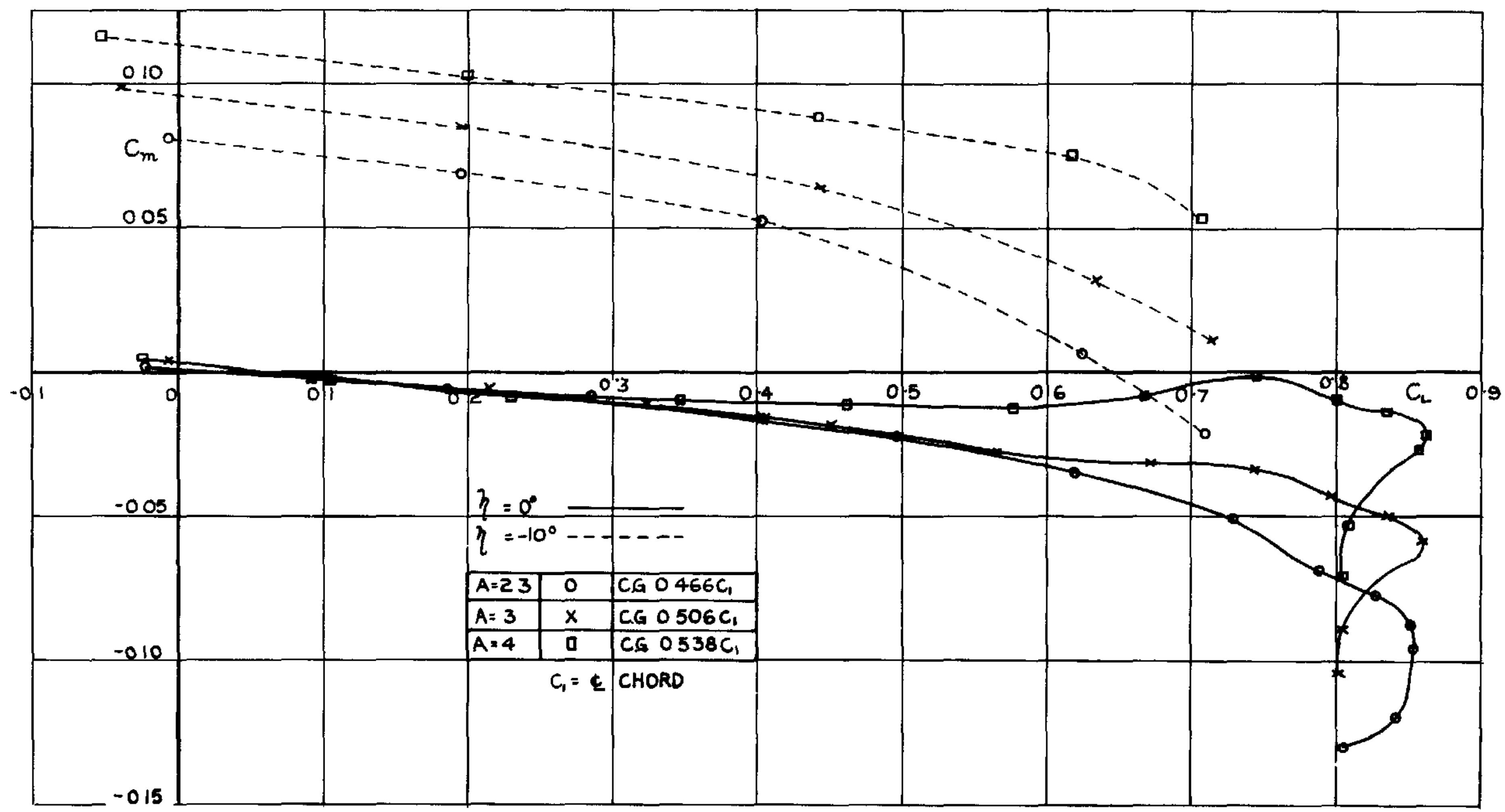

[C.G. POSITIONS ADJUSTED TO GIVE CONSTANT STABILITY AT $C_L = 0$]

WITH BODY WITHOUT GROUND $\eta = 0°$ AND $-10°$

PITCHING MOMENTS FOR WINGS OF VARIOUS ASPECT RATIOS.

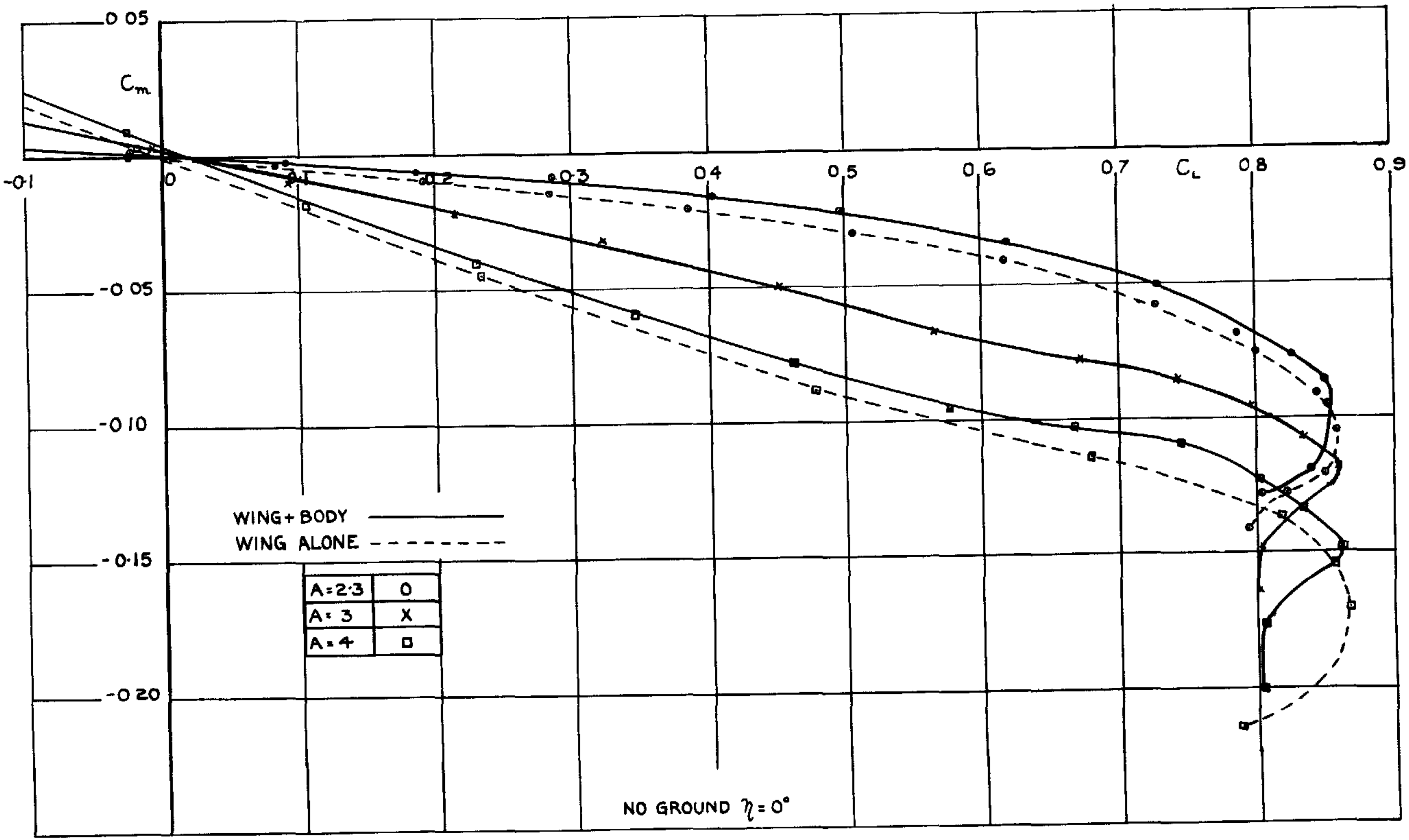

BODY EFFECTS ON PITCHING MOMENTS

FIG. 9

FIG. 10.

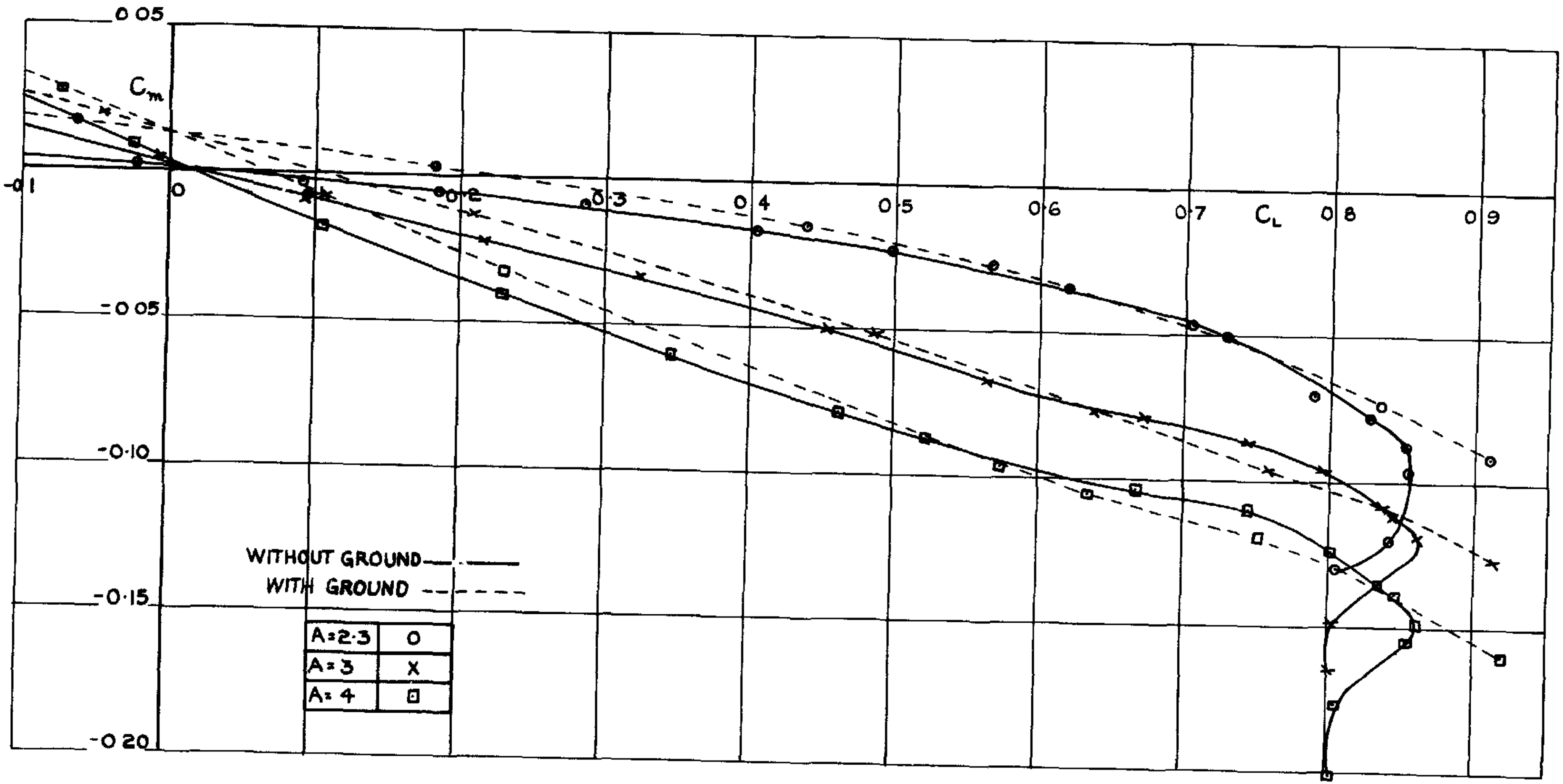

WITH BODY $\eta = 0°$

EFFECT OF GROUND ON PITCHING MOMENTS.

FIG.11

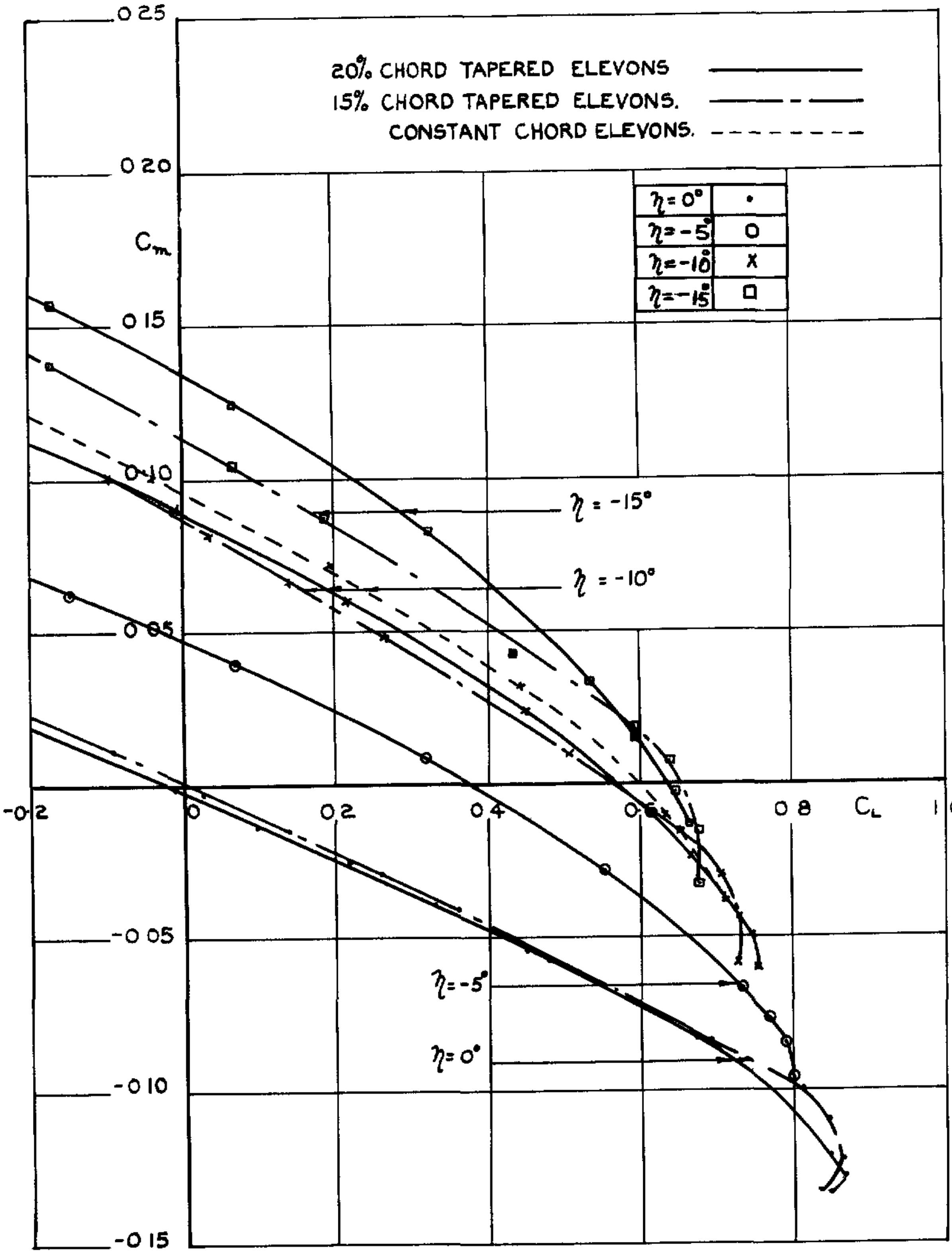

A = 3 WING + BODY. WITHOUT GROUND

EFFECT OF ELEVONS ON PITCHING MOMENTS.

FIG. 12.

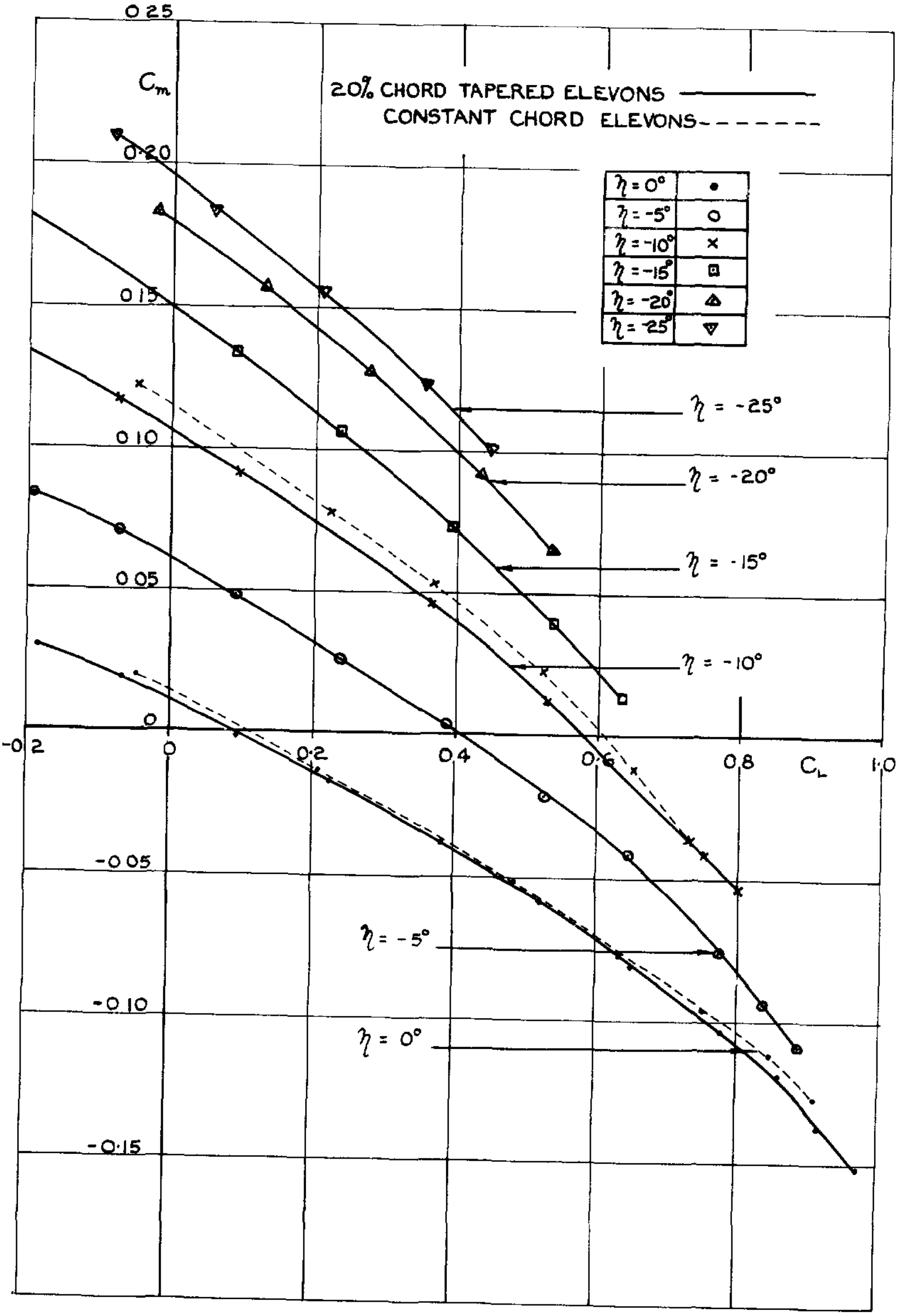

A = 3 WING + BODY

EFFECT OF ELEVONS ON PITCHING MOMENTS WITH GROUND.

FIG. 13.

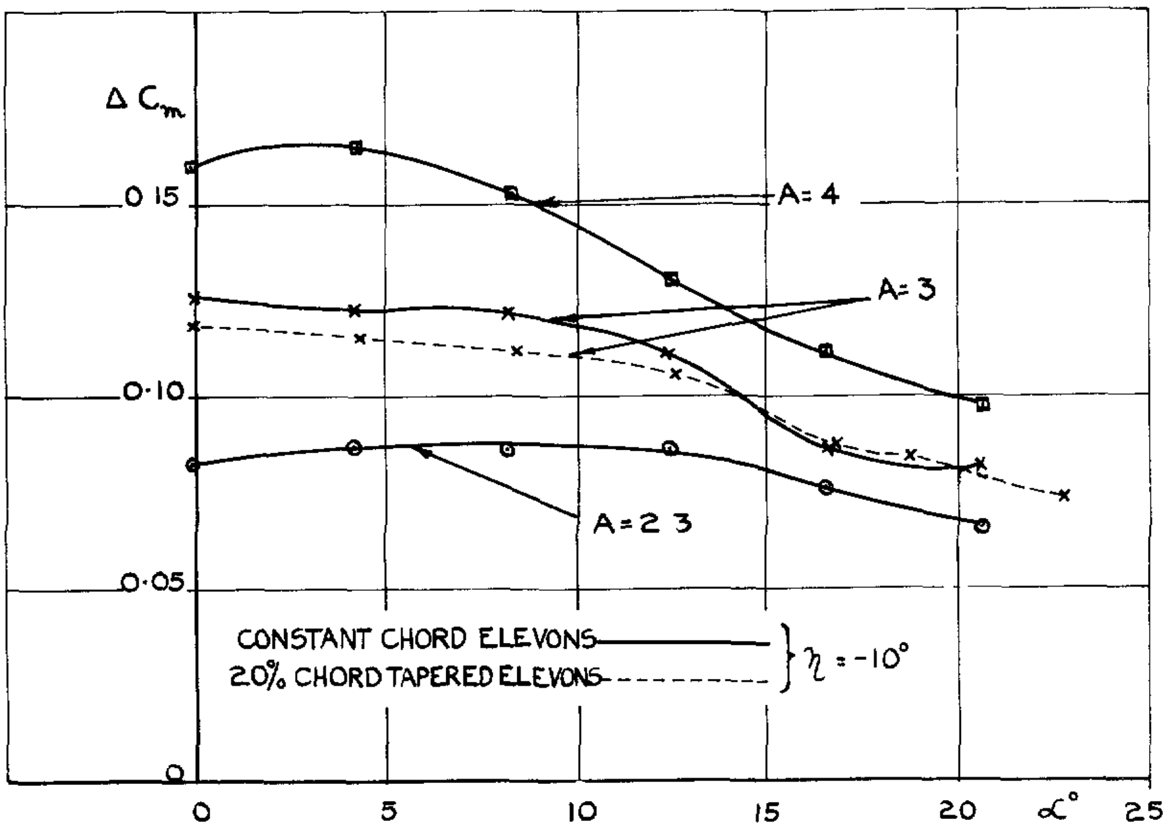

PITCHING MOMENT

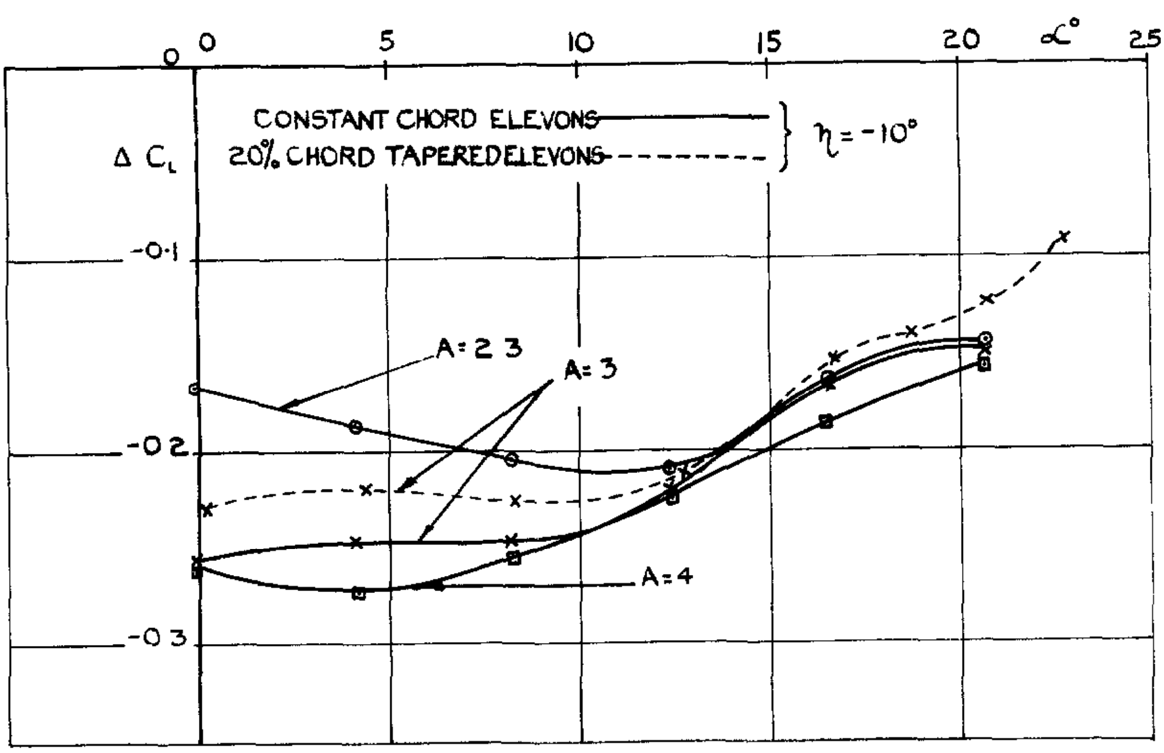

LIFT

BODY ON - WITHOUT GROUND

EFFECT OF ELEVONS AT CONSTANT INCIDENCE.

FIG. 14.

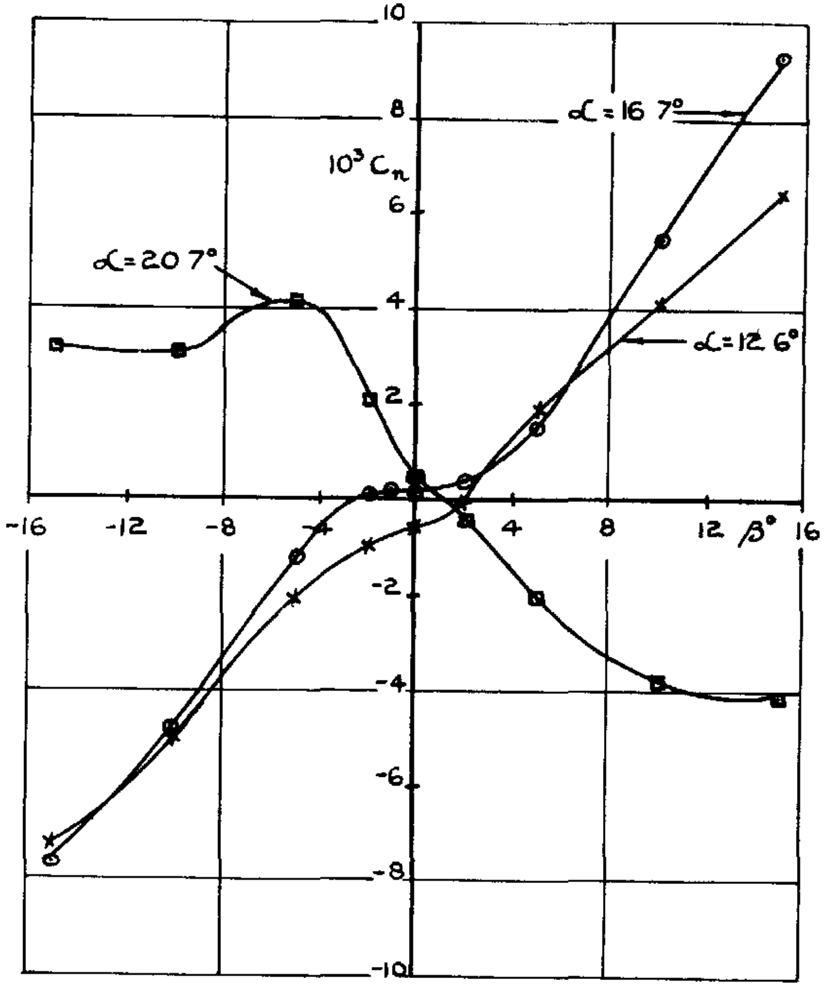

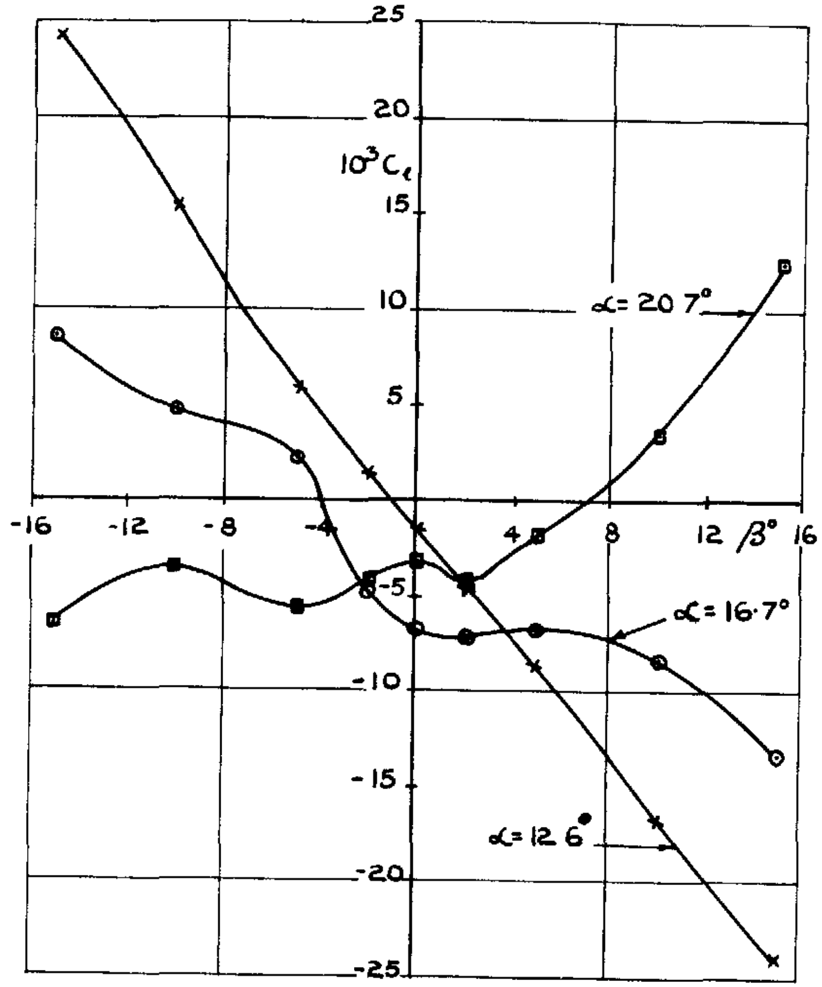

WING ALONE A=3

ROLLING AND YAWING MOMENTS DUE TO SIDESLIP.

FIG.15

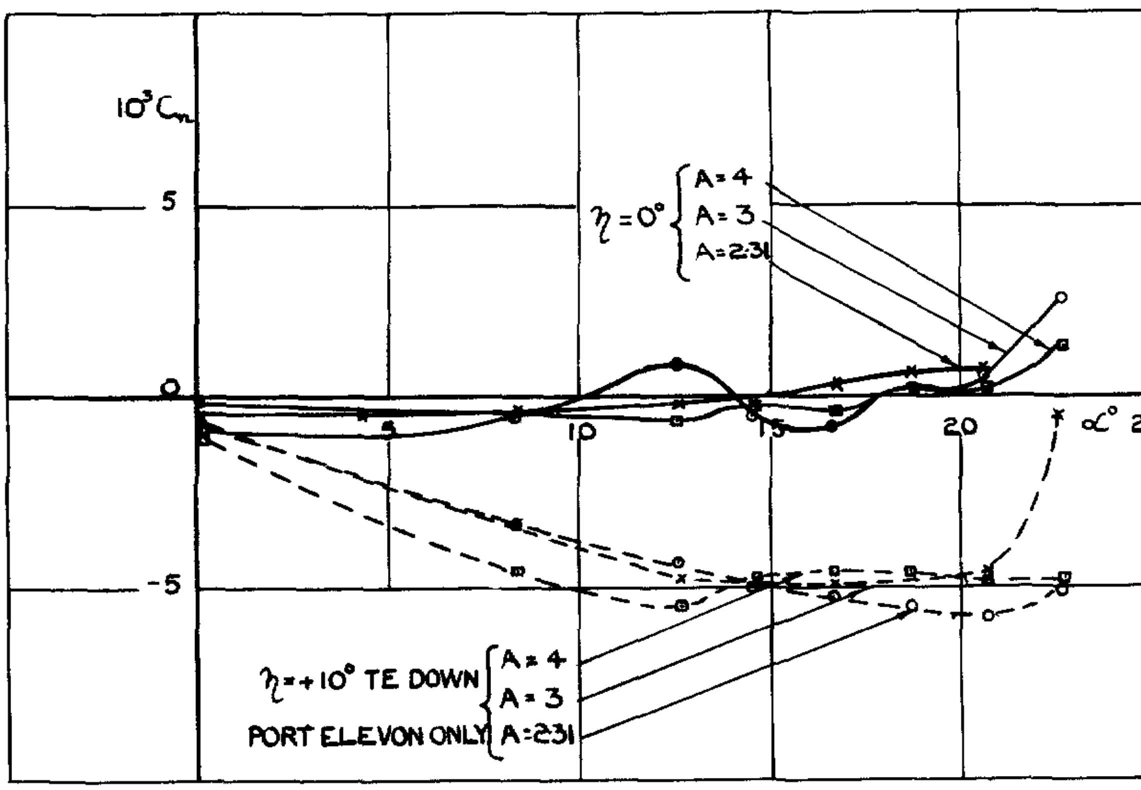

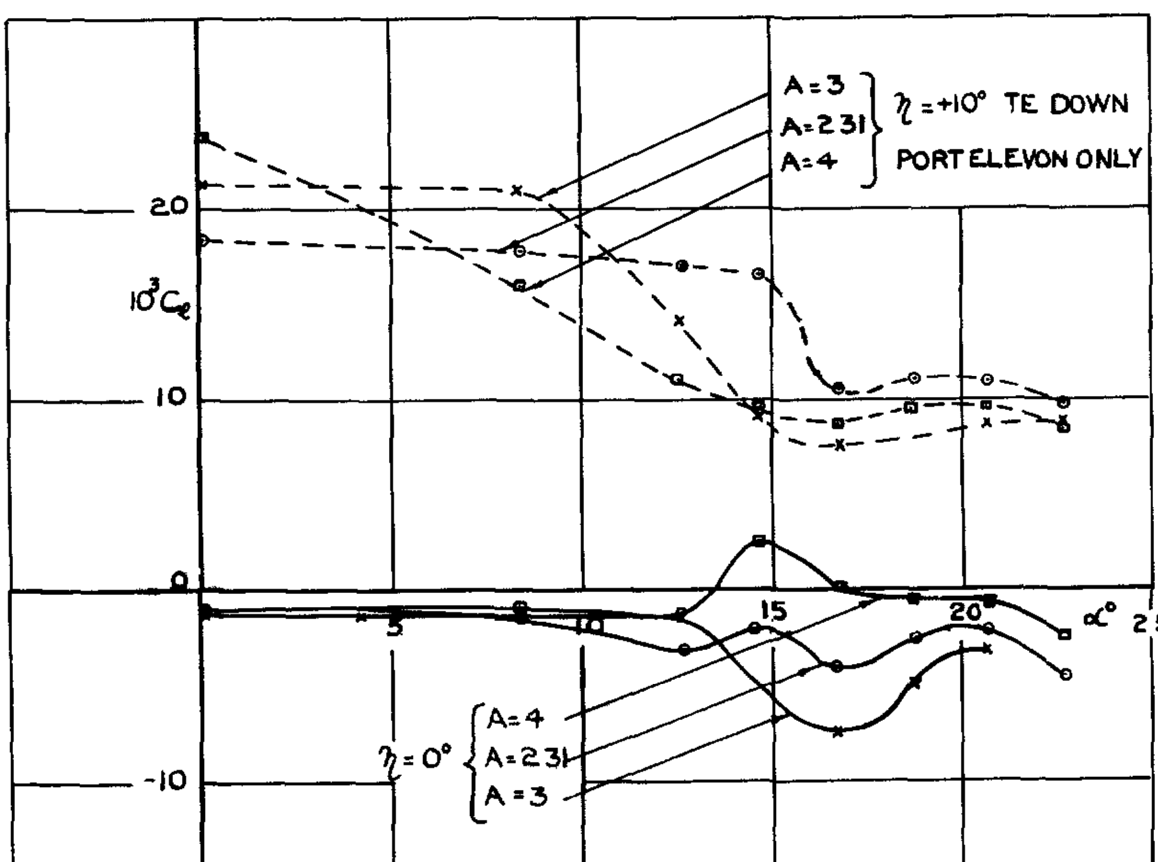

ZERO SIDESLIP CONSTANT CHORD ELEVONS
WING ALONE

EFFECT OF INCIDENCE ON ROLLING AND YAWING MOMENTS

FIG. 16.

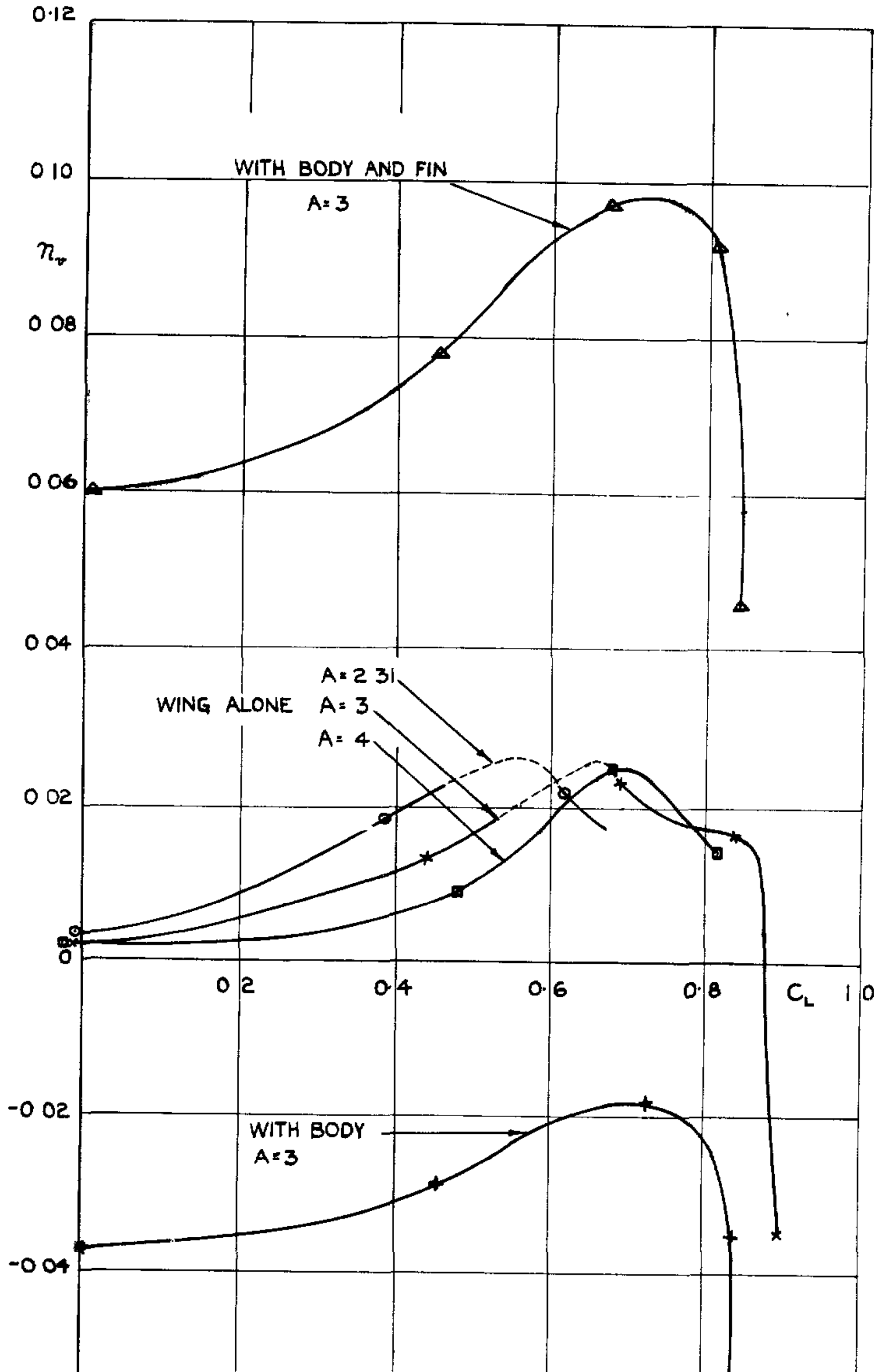

VARIATION OF n_v WITH LIFT.

FIG.17

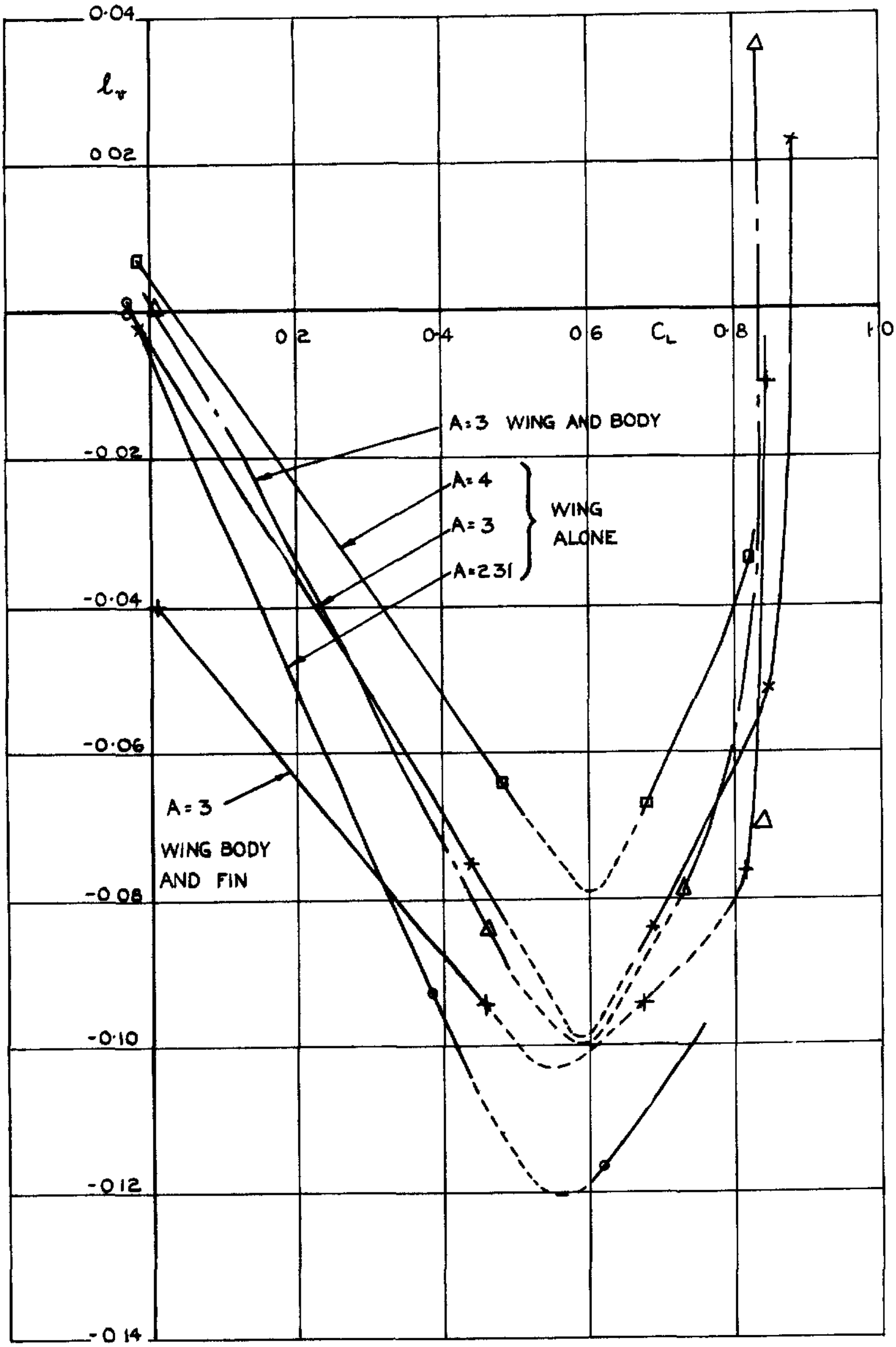

VARIATION OF ℓ_v WITH LIFT.

FIG. 18.

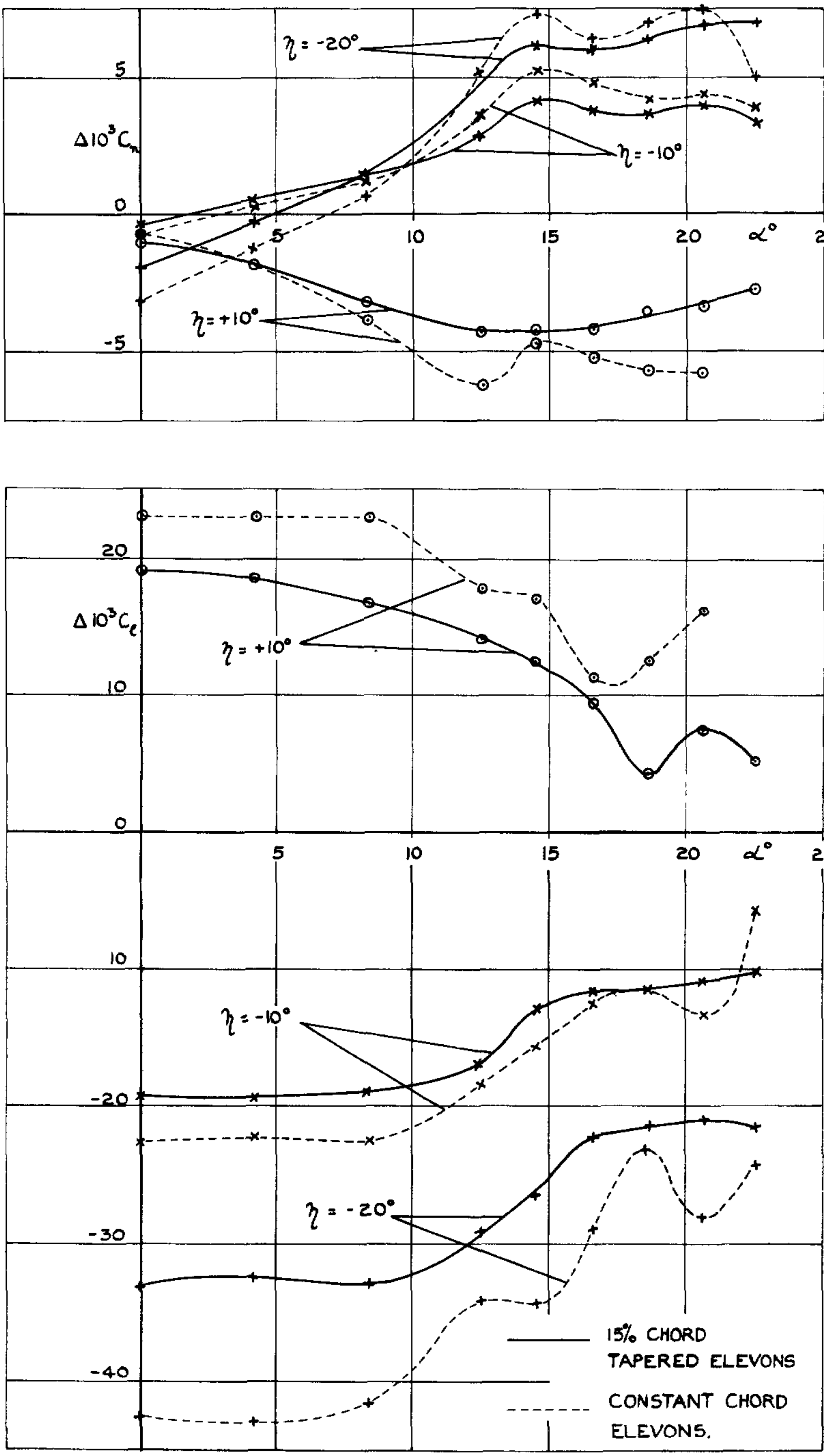

ZERO SIDESLIP A=3 PORT ELEVON ONLY η +ve T.E. DOWN

EFFECT OF ELEVON ON ROLLING AND YAWING MOMENTS.

C.P. No. 83

Report No. Aero. 2284
August, 1948

Wind Tunnel Tests on a 90°-Apex Delta Wing of Variable Aspect Ratio (Sweepback 36.8°)

Part II - Measurements of Downwash and Effect of High Lift Devices

by

R.C. Lock, B.A.

J.G. Ross, B.Sc.(Eng.), A.F.R.Ae.S.

and

P. Meiklem

SUMMARY

Wind tunnel measurements of downwash were made on Delta wings of aspect ratios 4, 3 and 2.3, using a tail of Delta planform in three vertical positions at two chordwise stations behind the wing. The tests also included the effect of the tail, and of split flaps and nose flaps, on the stability near the stall and on C_L max.

The tip nose flaps proved effective in delaying the tip stall, and gave some increase in C_L max. With split flaps untrimmed C_L max was 0.95 and 1.2 with the flap in the forward and rear position respectively. There was no change of trim with the flaps in the forward position with tail off; with the tail an intermediate flap position should give zero trim change.

The downwash was large at high lift coefficients, owing to the early tip stall, and this caused a loss of tail efficiency with a corresponding slight instability near the stall, which should not be serious.

A method is given of calculating the downwash at small incidences behind a Delta wing, and the results show good agreement with the measured values, provided that the experimental lift curve slope is used.

LIST OF CONTENTS

LIST OF APPENDICES

LIST OF TABLES

LIST OF ILLUSTRATIONS

1 Introduction

Extensive tests have already been made[1] in the No.2 $11\frac{1}{2}$ ft wind tunnel at the R.A.E. of longitudinal and lateral stability on some Delta wings. To complete the tunnel programme it was required to measure the downwash behind these wings, and to find the effect of a horizontal tail and of split flaps and nose flaps on the stalling characteristics. Some theoretical estimates of lift curve slope and downwash at low incidences were also made for comparison with the experimental results.

2 Description of model and test (See Table V, Fig.1)

The wing, which is more fully described in Ref.1, had a basic Delta planform of aspect ratio 4 and 90° apex angle, with the tips removable in two stages to give aspect ratios 3.0 and 2.31. The wing section was a 10% thick R.A.E.102 which has a L.E. radius of 0.685% C and maximum thickness at 35% C. No fuselage was used throughout these tests. The model was supported on the upper (three component) balance on three struts, using a rear sting to which the tail could be fixed. This was also of Delta planform, of aspect ratio 2.4, and could be fitted either on the sting or in two positions above it supported by a thin faired steel pillar. Two chordwise positions were available, giving six possible tail positions (of which only five were in fact used).

The model is shown in Fig.1, and relevant dimensions are given in Table V.

Lift, drag and pitching moments were measured on the three wings without tail and for a number of tail positions, at a wind speed of 200 ft/sec., giving Reynolds numbers of 2.7, 2.4 and 2.1×10^6 based on the mean chords for the three aspect ratios. Three tail settings $\eta_T = 0^\circ$, -4° and -8° were used in each case for the downwash measurements. Tests were included with 60° split flaps, of constant chord equal to $0.15\ C_R$ and of total span $1.0\ C_R$ (C_R = centre line chord), fitted in two positions:- at the trailing edge and one flap chord ahead of it. Tests were also made without tail to find the effect of nose flaps on lift and pitching moments (for the wing of aspect ratio 3 only). Two types were tried, each with a flap angle 130°. The first, covering the inboard half of the wing, had a chord (measured parallel to the plane of symmetry of the wing) equal to 10% of the local wing chord; the second, which extended from the tips over the outboard half of the wing, was of constant chord equal to 4% of the wing centre line chord. Both types were tested with and without split flaps.

The tests were made in the No.2 $11\frac{1}{2}$ ft $\times$ $8\frac{1}{2}$ ft wind tunnel at the R.A.E. during March and April 1948. The usual corrections for blockage and tunnel constraint have been applied to all the results quoted.

3 Discussion of results

3.1 Effect of high lift devices

The lift, drag and pitching moments for the wing of aspect ratio 3 (without tail) fitted with various flap combinations are given in Table VI; the lift curves are shown in Fig.2 and the corresponding pitching moment curves in Fig.3. The lift increments produced may be summarised as follows:-

TABLE I

Lift increments due to flaps

	ΔC_L at $\alpha = 10^\circ$	$\Delta C_{L_{max.}}$	α_{Stall} (= 21° for wing alone)
Nose flaps (inboard)	0	0.02	21°
" " (tip)	0	0.19	21°
Split flaps (rear position)	0.46	0.34	18°
" " (forward ")	0.30	0.08	16°
Split flaps (forward) with tip nose flaps	0.32	0.21	17°

Tuft observations showed that the tip nose flaps were successful in delaying the tip stall, but the inboard flaps had very little effect and are unlikely to be of any use. The rear position of the split flaps produced the greatest lift increment, but also caused a large nose down trim change without tail ($\Delta C_M = -0.12$). Moving the flap forward reduced this to zero, but also reduced the lift increments and brought about an early tip stall. This was to a large extent cured by the tip nose flaps, and it is thought that this combination should prove the most effective in practice for a tailless Delta. Fig.3 shows that there is a slight instability near the stall in this case only, but this did not occur until an incidence of 14° was reached and should not be serious.

A horizontal tail, however, causes a nose up pitching moment at constant C_L with the flaps in the forward position (see Fig.6) and it is probable therefore that an intermediate flap position will give zero trim change in this case.

3.2 Downwash measurements

In order to obtain the angle of downwash at a given wing incidence α, the pitching moments measured with the three tail settings are plotted against η_T, and from this curve the value of η_T for which C_M (tail on) = C_M (no tail) can be interpolated. The downwash angle ε is then given by $\varepsilon = \alpha + \eta_T$. The angle thus obtained is strictly a mean of the actual downwash angles over the area of the tail, but in fact should not differ appreciably from the value at the middle point of the tail root chord, which is close to the mean quarter chord point of the tail.

These values of ε (corrected for tunnel constraint) at various positions behind the wing are given in Tables X and XI and are plotted against incidence in Figs.7 - 9; they include the effects of split flaps. The most important feature of the results is that they show a large increase in downwash at angles of incidence near the stall, in almost all cases. This is so marked that the tail efficiency factor $(1 - \frac{d\varepsilon}{d\alpha})$ becomes negative at angles of incidence above about 15° (no flaps) or 12° (with flaps). The effect is due to the concentration of lift near the centre of the wing at high lift coefficients produced by the early tip stall, which causes a correspondingly large downwash downstream in the wake. The only exception occurs in the rear lowest position of the tail on the sting, which at high incidences is below the wake, so that the downwash is much smaller here than at the other positions.

3.3 Effect of the tail on longitudinal stability

Lift and pitching moment coefficients with tail are given in Tables VII, VIII and IX and some $C_M - C_L$ curves are shown in Figs.4 and 5 (tail in rear position), and in Fig.6 (tail in forward position). The C.G. position for these curves differs from that used in Fig.3 (tail off) and in Ref.1; it was chosen to give a reasonable static margin at low incidences. It will be seen that the loss of tail effectiveness near the stall, due to the large downwash at the tail, causes a definite instability at lift coefficients above about 0.8 (no flaps), 0.85 (flaps in forward position), or 1.0 (flaps in rear position). The lowest rear position of the tail (Fig.5) is the only one which avoids this trouble; but even in the other cases the instability should not be very serious, as it is small and only occurs just before the stall.

The control power of the tail $\left(\frac{dC_M}{d\eta_T}\right)_{\alpha=0^o}$ under various conditions is given below in Table II. The loss of control power near the stall is very small (see Fig.4), and there is no change due to putting flaps down.

TABLE II

Control Power of the Tail

Condition		$\left(\frac{\partial C_M}{\partial \eta_T}\right)_{\alpha = 0^o}$ per degree
Rear tail position		
A = 2.31	Low tail position	- 0.0074
	Middle tail position	- 0.0083
	High " "	- 0.0085
A = 3	Middle tail position	- 0.00875
A = 4	" " "	- 0.0099
Forward tail position		
A = 3	Middle tail position	- 0.0057
	High " "	- 0.0060

4 Theoretical estimation of lift curve slope and downwash (see also Appendix)

Calculations have recently been made of the downwash behind sweptback wings of large aspect ratio (Ref.2), and behind wings of small aspect ratio with zero sweep (Ref.3), but up to the present nothing has been published for swept-back or Delta wings of small aspect ratio. It was therefore decided to make an independent calculation for these particular Delta wings, using an extension of Wieghard's method for rectangular wings (see Ref.3).

The continuous chordwise distribution of vorticity over the wing is represented by four kinked horseshoe vortices (see Fig.11b), and the assumption is made that the spanwise lift distribution is elliptical; Falkner (Ref.4) has shown that this should be a good approximation for the wings of aspect ratio 2.3 and 3, but less good for that of aspect ratio 4. The downwash due to these vortices is evaluated at four points on the wing centre line and is equated to the angle of incidence of the wing; hence four simultaneous equations are obtained from which the strengths of the four vortices can be calculated. Details of the method are given in the appendix.

The lift curve slopes for the three wings thus obtained are tabulated below, together with the results of Falkner's paper[4] and of the wind tunnel tests[1].

TABLE III

Lift curve slopes. (per radian)

A.R.	$\frac{dC_L}{d\alpha}$ (4 vortex method)	$\frac{dC_L}{d\alpha}$ (Falkner)	$\frac{dC_L}{d\alpha}$ (measured)
2.31	2.47	2.76	2.69
3.0	2.92	3.14	3.15
4.0	3.52	3.47	3.44

The measured values all agree well with Falkner's calculations, but the results obtained by the four vortex method are low for the two smaller aspect ratios. This is probably due to the fact that the method does not take into account the singularity in the downwash which occurs at the kink of a swept vortex (see e.g. Ref.5). In order to allow for this it would be necessary to superimpose on the original elliptic distribution an additional vorticity function near the centre of the bound vortices, which would reduce the circulation and hence the downwash at points very close to the kink. The resulting lift curve slopes would thus be increased, and better agreement with experiment should be obtained. However, since the effect of this 'middle function' dies out rapidly behind the kink, there is no reason why the simple method should not give a good approximation to the downwash some distance behind the wing, provided that the measured values of the lift curve slopes are substituted for the incorrect calculated values.

When the relative strengths of the four kinked vortices are known, the downwash can easily be calculated at any point in the plane of symmetry of the wing. This has been done for the positions at which the downwash has been measured experimentally. These values of $\left(\frac{d\varepsilon}{d\alpha}\right)_{\alpha=0^\circ}$ are given in the first column of Table IV below. The second column gives the values obtained by using the measured lift curve slopes, and these are plotted against $\zeta = \frac{z}{s}$ (z = vertical height of tail above model $\mathbb{C}_L$, s = semi span) in Fig.10, together with the experimental results.

TABLE IV

Downwash at small incidences

	ζ	$\frac{d\varepsilon}{d\alpha}$ (calculated)	$\frac{d\varepsilon}{d\alpha}$ (calculated, assuming measured value of $\frac{dC_L}{d\alpha}$)	$\frac{d\varepsilon}{d\alpha}$ (measured)
A = 2.31 Rear tail position	0 0.227 0.455	0.73 0.58 0.44	0.79 0.63 0.48	0.77 0.65 0.50
A = 3.0 Rear tail position	0 0.194 0.389	0.68 0.56 0.44	0.74 0.61 0.48	- 0.615 -
A = 3.0 Forward tail "	0 0.194 0.389	0.77 0.62 0.47	0.83 0.67 0.51	- 0.65 0.55
A = 4.0 Rear tail position	0.167	0.54	0.53	0.58

There is good agreement with experiment in almost all cases, provided that the experimental lift curve slope is used in calculating the downwash. It is interesting to note that the calculated values for $\zeta \neq 0$, at the rear position, agree closely with Multhopp's results (see Ref.4 para.3.4) for the downwash outside the vortex sheet at an infinite distance downstream, viz.

$$\frac{d\varepsilon}{d\alpha}(-\infty, 0, \zeta) = \frac{d\varepsilon}{d\alpha}(-\infty, 0, 0) - |\zeta| \cdot \frac{2}{\pi A} \cdot \frac{dC_L}{d\alpha} \text{ for elliptic loading}$$

This is however no longer true close to the wing (at the forward position).

5 Conclusions

The tip nose flaps should prove effective in delaying the tip stall, and in conjunction with split flaps (in the forward position for a tailless Delta, or in an intermediate position for a Delta with tail) should give a satisfactory C_L max. (between 1.1 and 1.2, according to flap position), without any appreciable change of trim.

The large downwash at high lift coefficients, due to the early tip stall, will cause a loss of tail efficiency and a corresponding slight instability near the stall, but this should not be serious.

The calculations of downwash at low incidences show good agreement with the measured values, and the method employed should therefore be a satisfactory one for the estimation of downwash behind Delta wings of small aspect ratio, provided that the lift curve slope is first determined either by experiment or by a more accurate lifting surface theory.

REFERENCES

No.	Author	Title, etc.
1	Ross, Hills & Lock	Six component wind tunnel measurements on a 90° apex. Delta wing of variable aspect ratio (sweepback 36.8°). Part I - General Stability. (See Part I of this Report).
2	Schlichting	Calculations of the downwash behind sweptback wings of large aspect ratio (Part I). ARC.12,415, May, 1947.
3	Schlichting	Calculations of the downwash behind wings of small aspect ratio with zero sweep. Part II. ARC 11,244. October, 1947.
4	Falkner	Preliminary calculations on Delta wings. 126 vortex, 6 point solutions. N.P.L. Preliminary Sheets.
5	Schlichting	The lift distribution of a swept-back wing of infinite aspect ratio. Part I. The Indirect Problem. ARC. 11,665. June, 1948.

APPENDIX I

Calculation of lift and downwash for a Delta wing

Downwash behind a kinked horseshoe vortex

We shall use the non-dimensional co-ordinates $\xi = \frac{x}{s}$, $\eta = \frac{y}{s}$, $\zeta = \frac{z}{s}$, where the system of axes is as shown in Fig.11a. Then the downwash velocity at a point P (x, 0, z) due to a kinked vortex of span 2s and of strength $\Gamma(\eta)$ per unit length in the direction of the y axis can be shown to be

$$w = \frac{1}{2\pi s}\int_0^1 -\frac{d\Gamma}{d\eta}\left[\frac{\eta}{\eta^2+\zeta^2} + \frac{\xi^2\sin\varphi\cos\varphi}{(\xi^2\cos^2\varphi+\zeta^2)\sqrt{\xi^2+\zeta^2}}\right.$$

$$\left. - \frac{1}{\sqrt{(\xi^2+\zeta^2+2\xi\eta\tan\varphi+\eta^2\sec^2\varphi)}}\left(\frac{\xi\eta+\eta^2\tan\varphi}{\eta^2+\zeta^2} + \frac{\xi\eta+\xi^2\sin\varphi\cos\varphi}{\xi^2\cos^2\varphi+\zeta^2}\right)\right] d\eta \qquad \text{..... (1)}$$

If the distribution of vorticity is elliptical, then Γ is of the form

$$\Gamma = 2Us\gamma\sqrt{1-\eta^2} \qquad \text{..... (2)}$$

so that

$$-\frac{d\Gamma}{d\eta} = 2Us\gamma\frac{\eta}{\sqrt{1-\eta^2}} \qquad \text{..... (3)}$$

Hence, substituting in (1),

$$\varepsilon(x,0,z) = \frac{w}{U} = \frac{\gamma}{\pi}\left[\frac{\pi}{2}\left(1-\frac{|\zeta|}{\sqrt{\xi^2+\zeta^2}}\right) + \frac{\xi^2\sin\varphi\cos\varphi}{(\xi^2\cos^2\varphi+\zeta^2)\sqrt{\xi^2+\zeta^2}} + I + J\right]$$

$$= \gamma \times a(\xi, \zeta, \varphi) \qquad \text{..... (4)}$$

where

$$I = -\int_0^1 \frac{\eta^2(\xi+\eta\tan\varphi)\,d\eta}{(\eta^2+\zeta^2)\sqrt{(1-\eta^2)(\xi^2+\zeta^2+2\xi\eta\tan\varphi+\eta^2\sec^2\varphi)}}$$

and

$$J = -\frac{\xi}{(\xi^2\cos^2\varphi + \zeta^2)} \int_0^1 \frac{\eta(\eta + \xi\sin\varphi\cos\varphi)\,d\eta}{\sqrt{(1-\eta^2)\,(\xi^2 + \zeta^2 + 2\xi\eta\tan\varphi + \eta^2\sec^2\varphi)}} \ .$$

When $\zeta = 0$, this reduces to

$$\varepsilon(x,0,0) = \frac{\gamma}{\pi}\left[\frac{\pi}{2} + \frac{\tan\varphi}{|\xi|} - \frac{1}{\xi\cos\varphi}\int_0^1 \frac{\sqrt{(\xi^2\cos^2\varphi + \xi\eta\sin 2\varphi + \eta^2)}}{\sqrt{1-\eta^2}}\,d\eta\right] \qquad (5)$$

(The <u>positive</u> value of ξ must be taken in the second term because the square root in the corresponding term of equation (4) is always positive.)

An explicit expression for the integrals occurring in equations (4) and (5) would be extremely complicated and involve elliptic integrals of the first and third kinds; but it is easy to evaluate them numerically in any particular case when the values of ξ, ζ and φ are known.

<u>Calculation of lift for Delta wings</u>

We make the assumption that the spanwise lift distribution is elliptical (see para.4). In order to represent the chordwise distribution of vorticity, the wing planform is split up into four equal strips (see Fig.11b), and a kinked vortex with elliptic distribution is placed along the quarter chord line of each of these strips. If the strengths of these vortices are given by $\gamma_1, \gamma_2, \gamma_3$ and γ_4 (see equation (2), and their angles of sweepback are φ_1, φ_2, φ_3, and φ_4 respectively, then the downwash at any point P $(x,0,z)$ is given by

$$\varepsilon = \sum_{i=1}^{4} a_i \gamma_i \qquad \ldots\ldots (6)$$

where

$$a_i = a(\xi_i, \zeta, \varphi_i), \quad \text{(see equation (4))},$$

and ξ_i is the non-dimensional co-ordinate of P with respect to the kink V_i of the i th vortex.

In this way the downwash angle is calculated at each of the four points P_i (Fig.11b), which are the $\frac{3}{4}$ chord points, on the centre line, of the four strips, and is equated to the angle of incidence α, thus giving four simultaneous equations for γ_i of the form

$$\sum_{j=1}^{4} a_{ij}\,\gamma_j = \alpha \ (i = 1,2,3,4) \qquad \ldots\ldots (7)$$

When the values of γ_i are known the lift can be found from the equation

$$\frac{2\,C_L}{\pi A} = \sum_{i=1}^{4} \gamma_i \qquad \text{.....}\ (8)$$

and the downwash at any point in the plane of symmetry of the wing can be calculated from equation (4).

TABLE V

Model Dimensions

Wing

R.A.E.102 (for ordinates see Ref.1)

Thickness/chord ratio		0.10		
Apex angle		90°		
Angle of sweepback ($\frac{1}{4}$ chord line)		36.9°		
Root chord, C_R - ft.		3.200		
		A=4.0	A=3.0	A=2.31
Span	b - ft	6.400	5.485	4.685
Mean chord	$\bar{C}$ - ft	1.600	1.818	2.028
Area	S - ft^2	10.24	9.97	9.50
Tip chord	- ft	0	0.458	0.858

Tailplane

Thickness/chord ratio	0.15
Root chord ($= \frac{1}{3} C_R$) - ft	1.067
Tip chord ($= \frac{1}{12} C_R$) - ft	0.267
Span - ft	1.600
Area - ft^2	1.067
Aspect ratio -	2.41
Distance of middle point of tail root chord behind middle point of wing root chord - ft	
Rear tail position	3.20
Forward tail position	2.133
Height of tail above wing ℄ - ft	
Middle position	0.533
High position	1.067

Split flaps

Flap angle	60°
Chord (= 15% C_R) - ft	0.480
Total span - ft	3.200
Distance of flap L.E. ahead of wing T.E. - ft	
Rear flap position	0.480
Forward flap position	0.960

Nose flaps

Tip flaps

Flap angle	130°
Chord (constant) - ft	0.125
Span (per flap) - ft	1.371

TABLE V (Ct'd)

Central flaps

Flap angle	130°
Chord - at tip - ft	0.150
- at root	0.333
Span (per flap) - ft	1.371

C.G. Positions - Distance aft of L.E. of ℄ chord - ft

Without tail (= 0.466 C_R)	1.493
With tail (= 0.525 C_R)	1.680

TABLE VI

A.R. = 3.00 C.G. at 0.466 C_R No Tail

Lift, Drag and Pitching Moment Coefficients

No Flaps			
α^o	C_L	C_D	C_M
0	-0.012	0.0069	0.0096
4.15	+0.215	0.0110	-0.0162
8.30	0.445	0.0278	-0.0459
12.45	0.665	0.0748	-0.0743
16.55	0.816	0.1654	-0.0778
18.60	0.846	0.2308	-0.1047
20.60	0.875	0.2862	-0.1269
22.60	0.867	0.3349	-0.1580

No Split Flaps Tip Nose Flaps			
α^o	C_L	C_D	C_M
-0.05	-0.042	0.0229	0.0097
4.15	+0.200	0.0199	-0.0162
8.30	0.440	0.0342	-0.0448
12.45	0.681	0.0628	-0.0744
16.60	0.888	0.1157	-0.0920
18.70	0.971	0.1790	-0.0978
20.75	1.062	0.2520	-0.1296
22.70	1.036	0.3174	-0.1410

Flaps in Forward Position			
α^o	C_L	C_D	C_M
0.30	0.436	0.1598	-0.0467
4.40	0.611	0.1754	-0.0659
8.55	0.790	0.2043	-0.0933
12.65	0.920	0.3047	-0.1095
16.65	0.954	0.3916	-0.1313
18.65	0.913	0.4465	-0.1395

Flaps in Forward Position with Tip Nose Flaps			
α^o	C_L	C_D	C_M
0.30	0.426	0.1684	-0.0461
4.45	0.617	0.1822	-0.0664
8.55	0.800	0.2062	-0.0875
12.70	0.975	0.2494	-0.1054
16.75	1.091	0.3220	-0.0981
18.75	1.061	0.3969	-0.0890

Flaps in Rear Position			
α^o	C_L	C_D	C_M
0.35	0.538	0.1649	-0.1742
4.50	0.743	0.1926	-0.1997
8.65	0.939	0.2489	-0.2300
12.80	1.129	0.3401	-0.2624
16.85	1.218	0.4627	-0.2854
18.85	1.211	0.5285	-0.2948

No Split Flaps With Inboard Nose Flaps			
α^o	C_L	C_D	C_M
0	-0.029	0.0308	-0.0321
4.15	+0.204	0.0214	-0.0423
8.30	0.434	0.0326	-0.0584
12.45	0.664	0.0745	-0.0770
16.55	0.824	0.1497	-0.0817
18.60	0.865	0.2096	-0.0885
20.60	0.892	0.2498	-0.1059
22.60	0.894	0.2827	-0.1208

TABLE VII

A = 2.31 Tail Rear No Flaps C.G. at 0.525 C_R

Lift and Pitching Moment Coefficients

No Tail		
α^o	C_L	C_M
0	-0.006	0.0072
4.15	+0.191	0.0183
8.25	0.392	0.0253
12.40	0.608	0.0274
16.55	0.813	0.0150
18.55	0.861	0.0061
20.55	0.865	-0.0077
22.55	0.858	-0.0307

$\eta_T = -4^o$ Low Tail		
α^o	C_L	C_M
0	-0.028	0.0371
4.10	+0.174	0.0415
8.25	0.381	0.0383
12.40	0.615	0.0250
16.55	0.830	-0.0098
18.55	0.872	-0.0262
20.60	0.902	-0.0541
22.60	0.914	-0.0824

$\eta_T = 0^o$ Middle Tail		
α^o	C_L	C_M
0	-0.010	0.0117
4.15	+0.197	0.0088
8.25	0.405	0.0031
12.40	0.636	-0.0077
16.55	0.839	-0.0261
18.55	0.865	-0.0244
20.55	0.878	-0.0265
22.55	0.870	-0.0452

$\eta_T = -4^o$ Middle Tail		
α^o	C_L	C_M
0	-0.032	0.0453
4.10	+0.173	0.0424
8.25	0.381	0.0366
12.40	0.612	0.0264
16.55	0.809	0.0104
18.55	0.845	0.0096
20.55	0.859	0.0044
22.55	0.853	-0.0192

$\eta_T = -8^o$ Middle Tail		
α^o	C_L	C_M
-0.05	-0.057	0.0778
4.10	+0.150	0.0741
8.25	0.360	0.0683
12.40	0.588	0.0525
16.50	0.791	0.0412
18.55	0.824	0.0415
20.55	0.840	0.0333
22.55	0.839	0.0045

$\eta_T = -4^o$ High Tail		
α^o	C_L	C_M
0	-0.035	0.0459
4.10	+0.176	0.0377
8.25	0.390	0.0266
12.40	0.625	0.0129
16.55	0.812	0.0026
18.55	0.850	-0.0004
20.55	0.857	+0.0052
22.55	0.842	-0.0018

TABLE VIII

Rear Tail at Middle Height $\eta_T = -4^o$ C.G. at 0.525 C_R

Lift and Pitching Moment Coefficients

A = 2.31 No Flaps		
α^o	C_L	C_M
0	-0.032	0.0453
4.10	+0.173	0.0424
8.25	0.381	0.0366
12.40	0.612	0.0264
16.55	0.809	0.0104
18.55	0.845	0.0096
20.55	0.859	0.0044
22.55	0.853	-0.0192

A = 2.31 Flaps in Forward Position		
α^o	C_L	C_M
0.25	0.369	0.0907
4.35	0.536	0.0805
8.45	0.704	0.0755
12.60	0.883	0.0631
16.60	0.923	0.0655
18.60	0.887	0.0537

A = 3.00 No Flaps		
α^o	C_L	C_M
-0.05	-0.041	0.0413
4.15	+0.198	0.0302
8.30	0.436	0.0081
12.45	0.665	-0.0112
16.55	0.813	-0.0076
18.60	0.851	-0.0189
20.60	0.874	-0.0308
22.60	0.859	-0.0641

A = 2.31 Flaps in Rear Position		
α^o	C_L	C_M
0.30	0.463	-0.0086
4.45	0.658	-0.0158
8.55	0.846	-0.0249
12.70	1.076	-0.0411
16.80	1.211	-0.0449
18.80	1.198	-0.0428

A = 4.00 No Flaps		
α^o	C_L	C_M
-0.05	-0.040	0.0588
4.15	+0.209	0.0240
8.35	0.455	-0.0094
12.50	0.665	-0.0255
16.60	0.822	-0.0324
18.60	0.858	-0.0374
20.65	0.884	-0.0596
22.65	0.877	-0.0859

A = 3.00 Flaps in rear position		
α^o	C_L	C_M
0.30	0.469	-0.0244
4.50	0.690	-0.0474
8.60	0.895	-0.0723
12.75	1.090	-0.0891
16.80	1.178	-0.0888
18.80	1.174	-0.0882

TABLE IX

A = 3.00 Tail Forward $\eta_T = -4^\circ$ C.G. at 0.525 C_R

Lift and Pitching Moment Coefficients

No Flaps High Tail		
α°	C_L	C_M
-0.05	-0.045	0.0380
4.15	+0.198	0.0214
8.30	0.434	0.0020
12.45	0.670	-0.0146
16.60	0.841	-0.0270
18.60	0.877	-0.0244
20.60	0.884	-0.0348
22.60	0.868	-0.0520

No Flaps Middle Tail		
α°	C_L	C_M
-0.05	-0.051	0.0370
4.15	+0.194	0.0236
8.30	0.418	0.0087
12.45	0.651	-0.0045
16.55	0.831	-0.0163
18.60	0.866	-0.0133
20.60	0.873	-0.0248
22.60	0.859	-0.0430

Forward Flaps High Tail		
α°	C_L	C_M
0.25	0.371	0.0568
4.40	0.574	0.0409
8.55	0.766	0.0204
12.65	0.911	0.0128
16.65	0.919	0.0150
18.60	0.854	0.0036

Forward Flaps Middle Tail		
α°	C_L	C_M
0.25	0.365	0.0712
4.35	0.534	0.0620
8.50	0.726	0.0441
12.60	0.875	0.0380
16.60	0.886	0.0474
18.60	0.863	0.0188

Rear Flaps High Tail		
α°	C_L	C_M
0.30	0.470	-0.0541
4.50	0.689	-0.0719
8.60	0.895	-0.0943
12.75	1.097	-0.1056
16.80	1.176	-0.1070
18.80	1.160	-0.1235

Rear Flaps Middle Tail		
α°	C_L	C_M
0.30	0.434	-0.0317
4.45	0.648	-0.0451
8.60	0.861	-0.0654
12.75	1.062	-0.0702
16.80	1.148	-0.0571
18.80	1.138	-0.0866

TABLE X

A = 2.31 Downwash at Rear Tail Position

No Flaps		ε^{o}		
α^{o}	$C_{L_{Wing}}$	High Tail	Middle Tail	Low Tail
0	-0.006	0.5	0.5	0
4.1	+0.191	2.5	3.1	3.3
8.3	0.392	4.7	6.0	6.2
12.4	0.608	7.0	8.5	8.3
16.5	0.813	11.6	12.2	9.7
18.6	0.861	14.5	15.4	11.0
20.6	0.865	18.6	18.5	11.1
22.6	0.858	23.7	20.7	11.2

Forward Flaps		ε^{o}	
α^{o}	$C_{L_{Wing}}$	High Tail	Middle Tail
0.3	0.434	5.6	7.0
4.4	0.582	7.2	9.1
8.5	0.740	9.1	11.4
12.6	0.911	11.8	14.6
16.6	0.957	18.0	20.7
18.6	0.918	24.7	23.3

Rear Flaps		ε^{o}	
α^{o}	$C_{L_{Wing}}$	High Tail	Middle Tail
0.3	0.533	6.1	5.5
4.4	0.714	8.2	7.9
8.6	0.889	10.6	10.7
12.7	1.120	14.0	16.3
16.8	1.248	19.1	21.3
18.8	1.229	23.5	24.5

TABLE XI

Downwash Angles

No Flaps A = 3.00		ε^{o}		
α^{o}	$C_{L_{Wing}}$	Forward Position		Rear Position
		High Tail	Middle Tail	Middle Tail
0	-0.012	0.7	0.7	0.7
4.1	+0.215	3.0	3.4	3.1
8.3	0.445	5.3	6.1	5.7
12.5	0.665	7.7	8.8	8.4
16.6	0.816	11.4	12.8	12.5
18.6	0.846	14.6	15.8	14.9
20.6	0.875	18.4	20.2	17.6
22.6	0.867	21.8	24.5	18.9

No Flaps A = 4.00		ε^{o}
α^{o}	$C_{L_{wing}}$	Rear Position Middle Tail
0	-0.020	0.8
4.2	+0.221	3.2
8.3	0.450	5.7
12.5	0.664	8.6
16.6	0.816	12.2
18.6	0.850	14.6
20.6	0.875	16.6
22.6	0.867	18.9

Forward Flaps A = 3.00		ε^{o}	
α^{o}	$C_{L_{Wing}}$	Forward Position	
		High Tail	Middle Tail
0.3	0.436	5.9	10.0
4.4	0.611	7.9	12.3
8.5	0.790	9.9	14.9
12.6	0.920	12.9	17.6
16.7	0.954	18.8	24.7
18.6	0.913	22.2	27.9

Rear Flaps A = 3.00		ε^{o}		
α^{o}	$C_{L_{Wing}}$	Forward Position		Rear Position
		High Tail	Middle Tail	Middle Tail
0.3	0.538	6.5	8.3	7.6
4.4	0.743	8.5	10.1	9.7
8.6	0.939	10.9	13.3	12.2
12.7	1.129	14.2	16.7	15.7
16.8	1.218	19.5	21.9	21.1
18.8	1.211	23.8	24.7	24.7

Wt.2078.CP83.K3. Printed in Great Britain.

FIG. 1 a-c.

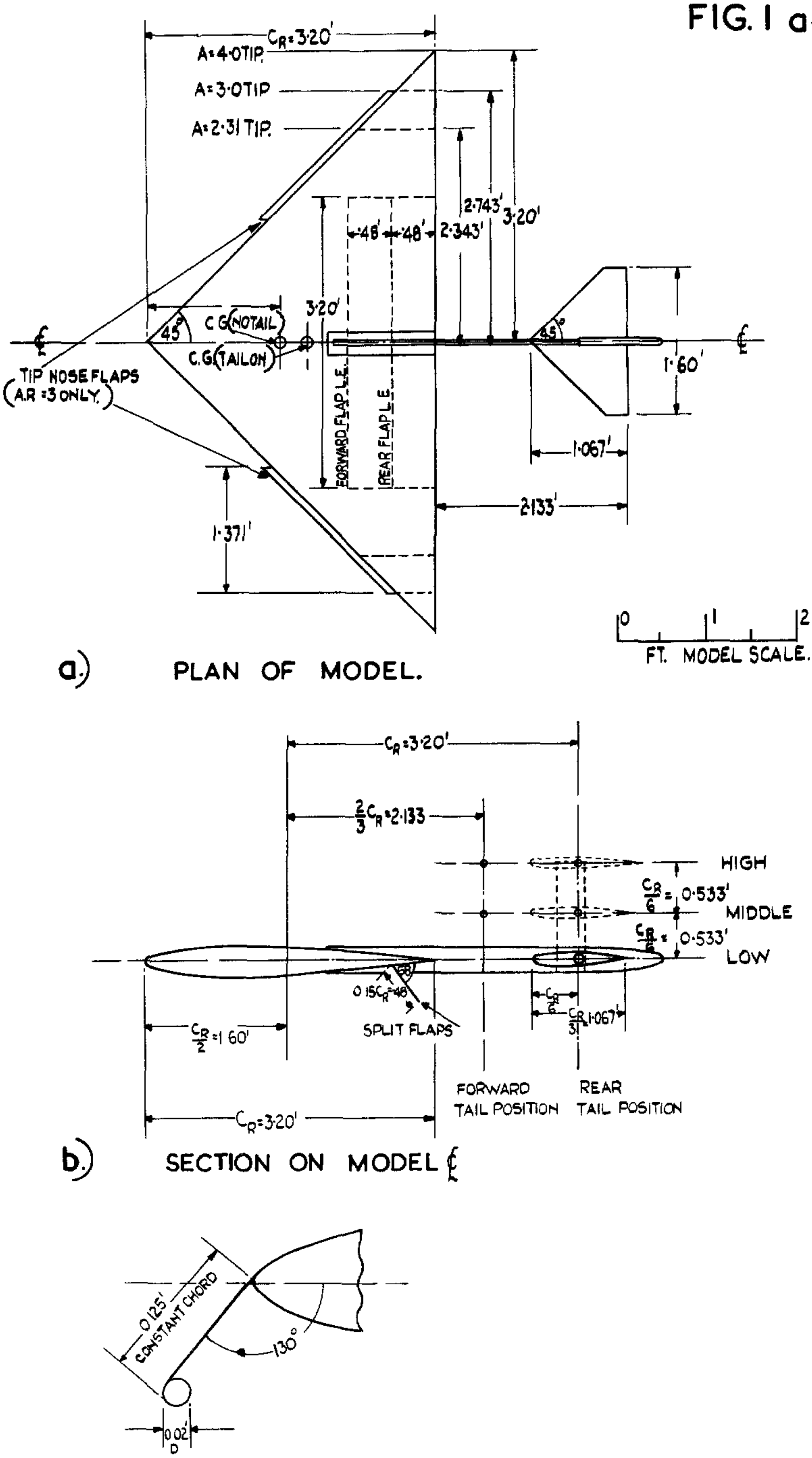

a.) PLAN OF MODEL.

b.) SECTION ON MODEL ℄

c.) TIP NOSE FLAPS.

FIG.1 (a-c) DELTA WING WITH TAIL.

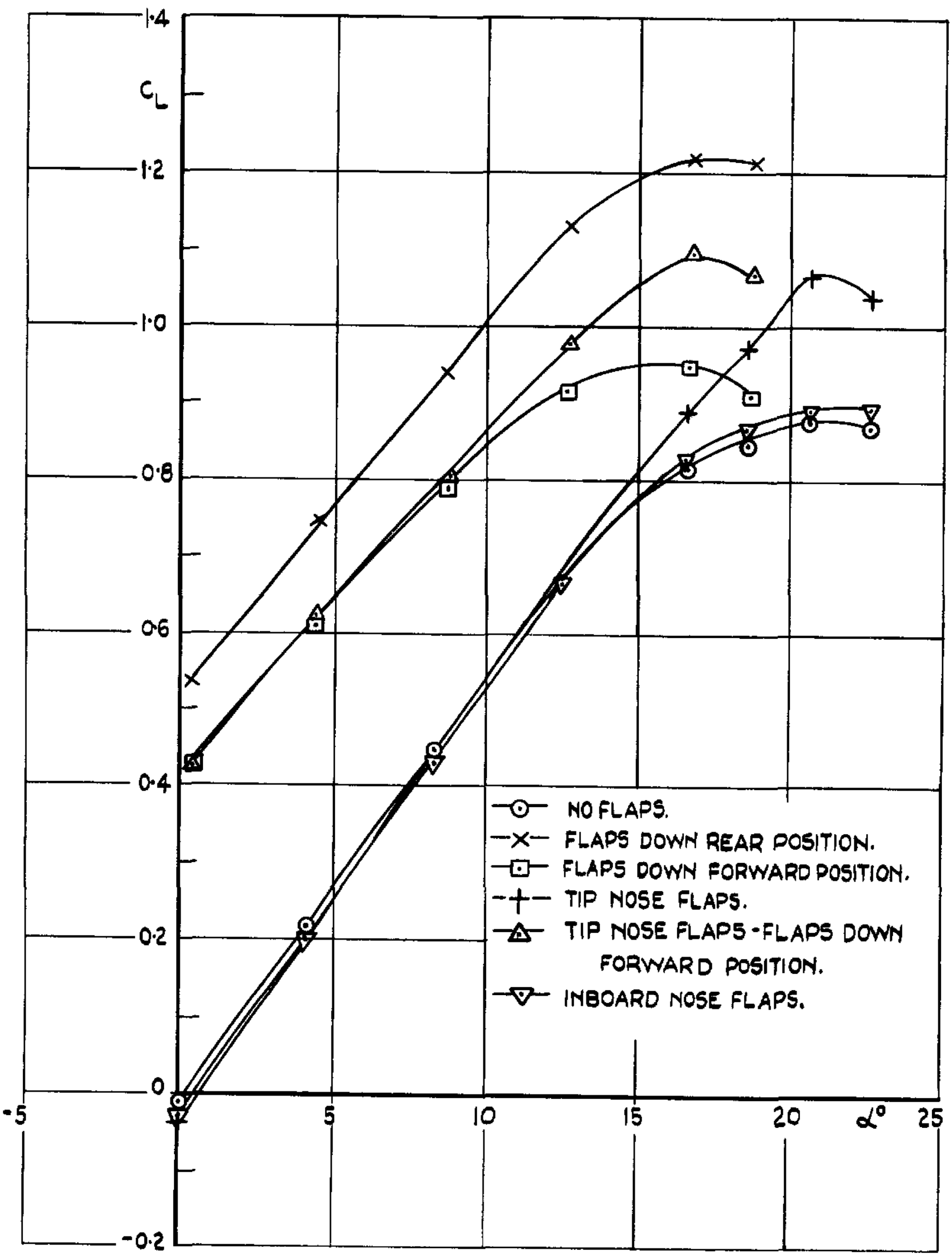

FIG. 2 LIFT COEFFICIENTS ON DELTA WING (WITHOUT TAIL). EFFECT OF HIGH LIFT DEVICES A.R. = 3.

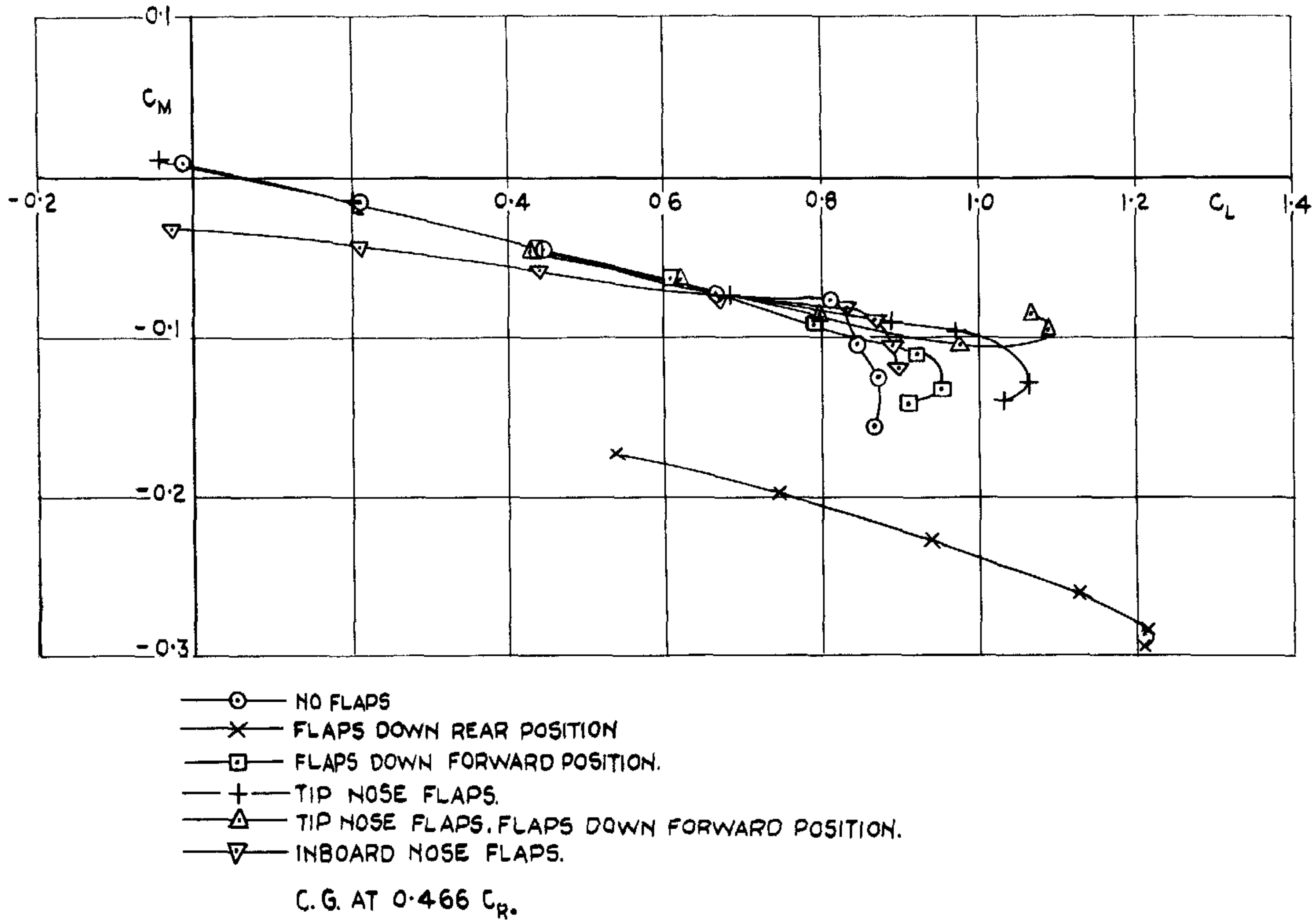

FIG.3 PITCHING MOMENT COEFFICIENTS ON DELTA WING (WITHOUT TAIL). EFFECT OF HIGH LIFT DEVICES AR=3.

FIG. 3

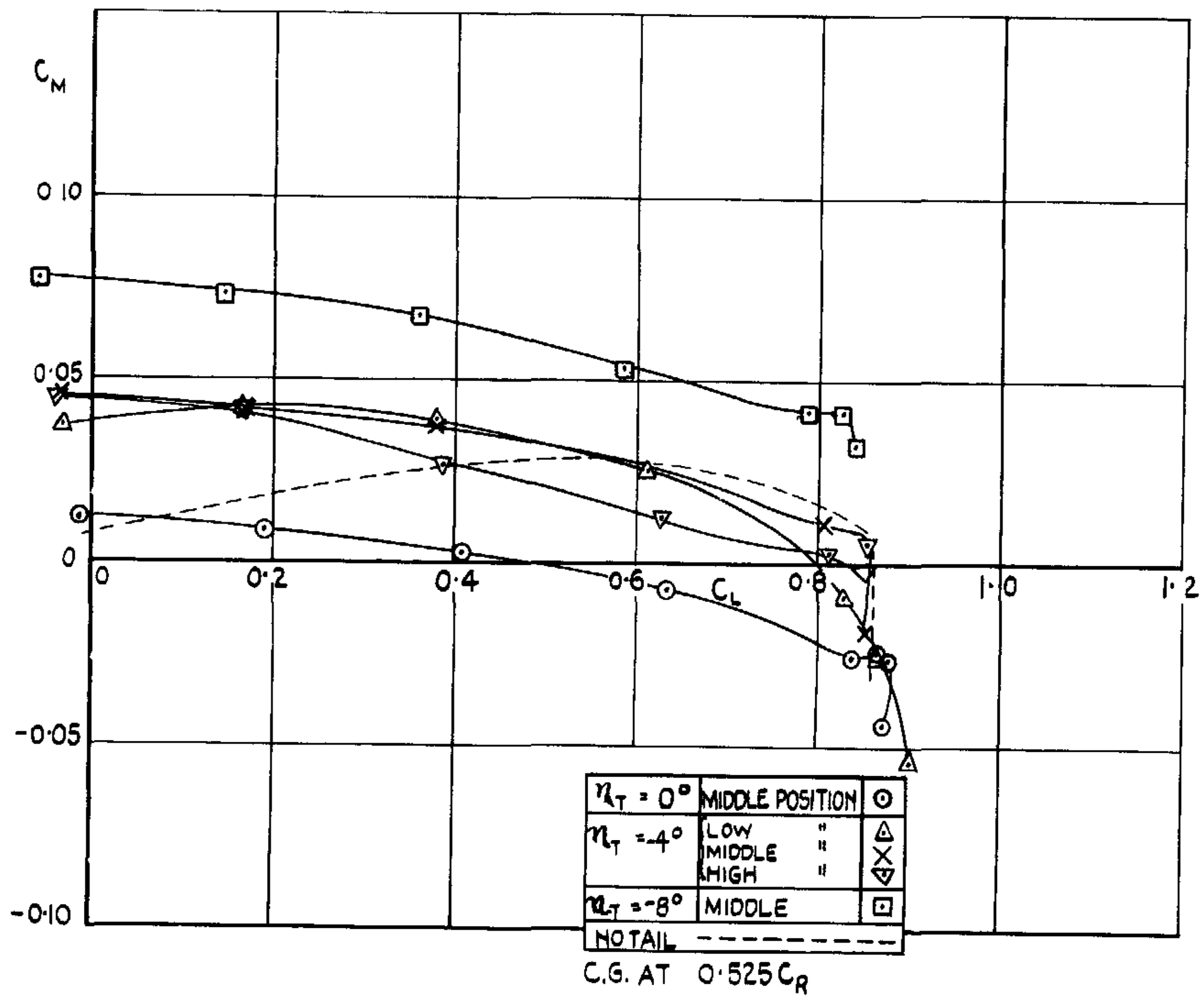

FIG.4 PITCHING MOMENT COEFFICIENTS ON A DELTA WING WITH TAIL. A.R. = 2·31 TAIL IN REAR POSITION.

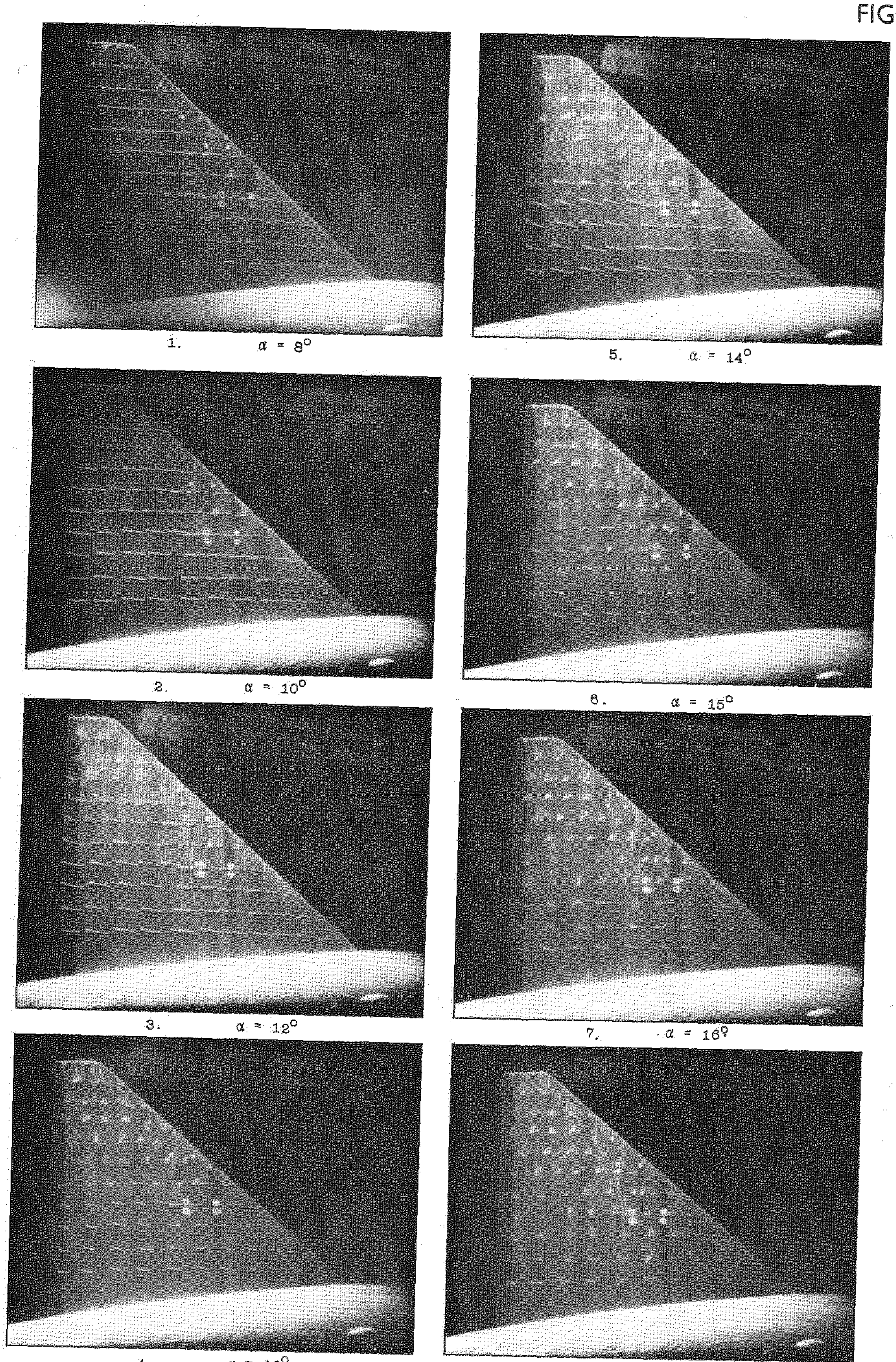

FIG.4. DELTA WING. 4E

TUFT PHOTOGRAPHS OF WING A = 2·31

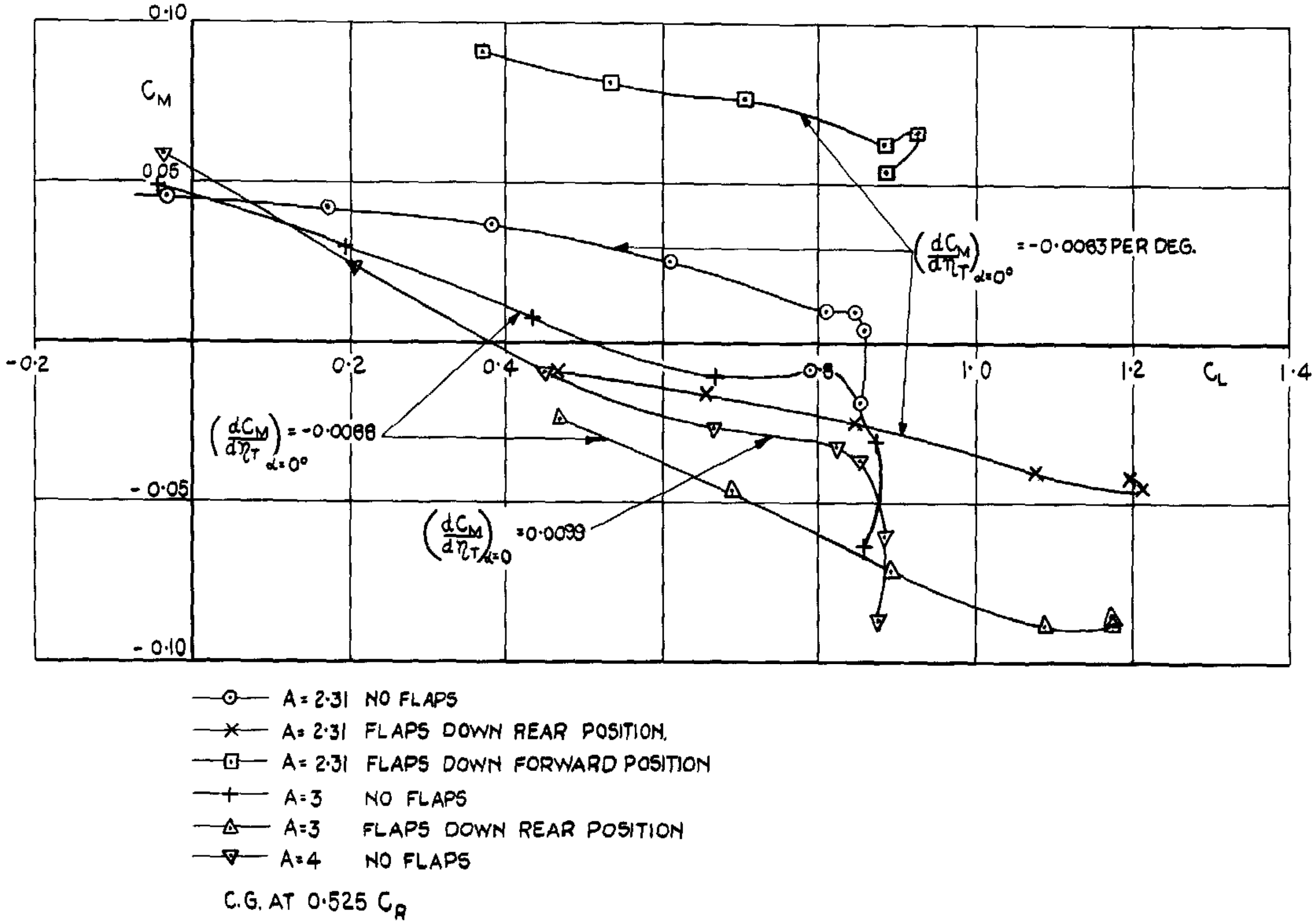

FIG.5. PITCHING MOMENT COEFFICIENTS ON DELTA WING WITH TAIL. TAIL IN REAR POSITION - MIDDLE TAIL POSITION - $\eta_T = -4°$

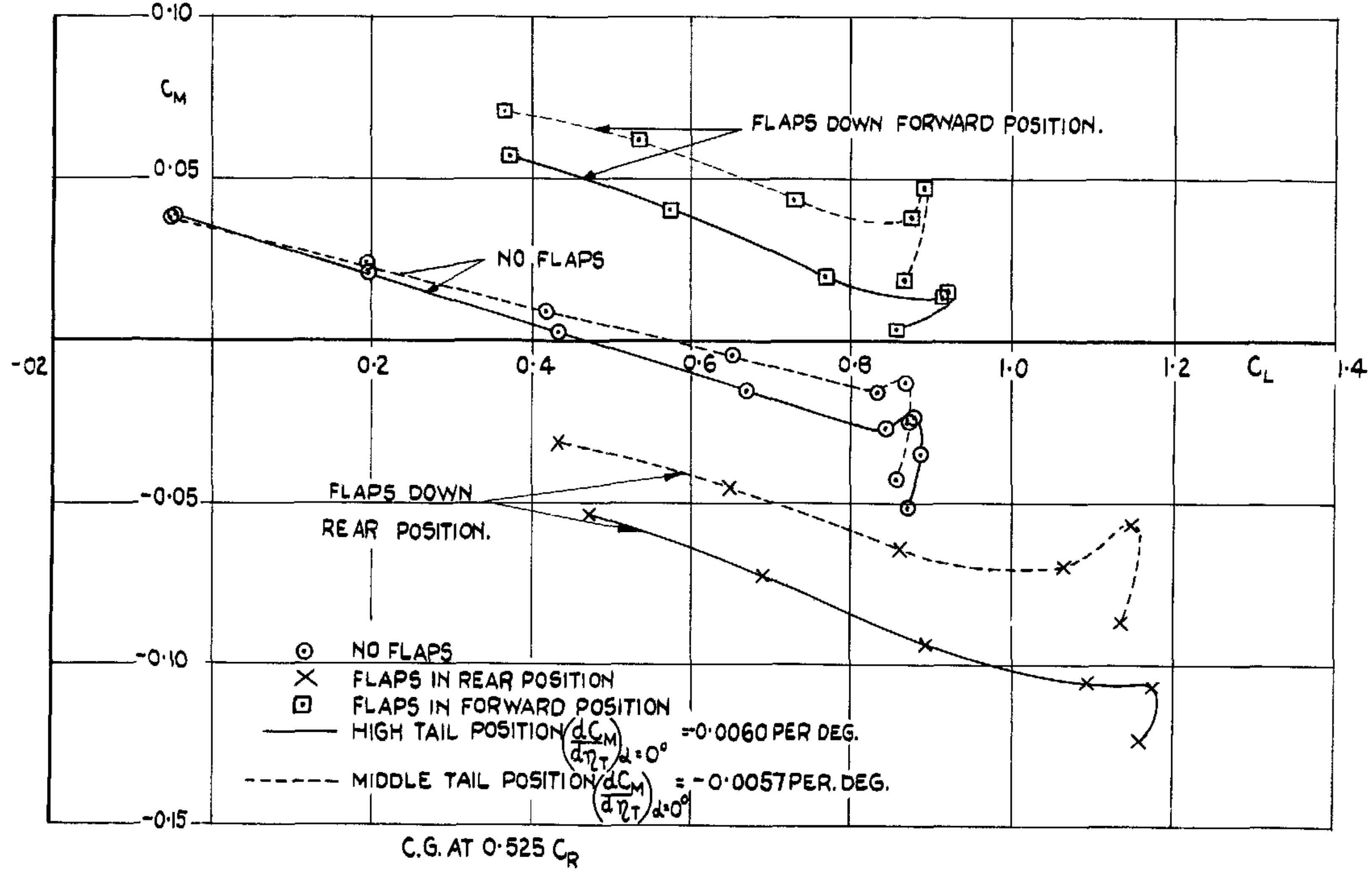

FIG.6 PITCHING MOMENT COEFFICIENTS ON DELTA WING (WITH TAIL).
TAIL IN FORWARD POSITION $\eta_T = -4°$ A.R = 3.

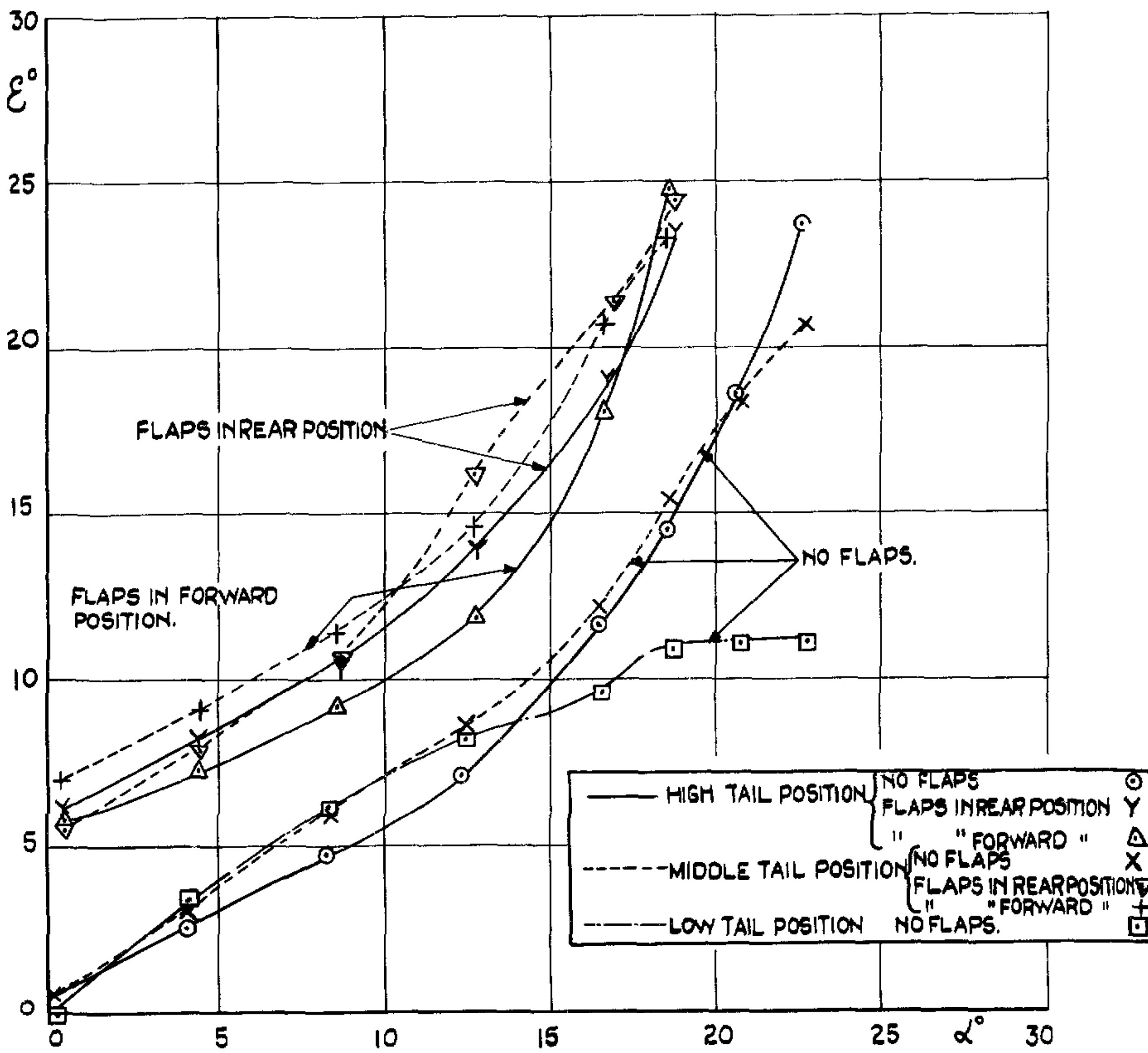

FIG. 7 DOWNWASH BEHIND A DELTA WING (WITH AND WITHOUT SPLIT FLAPS) A.R. = 2·31 TAIL IN REAR POSITION.

FIG. 8

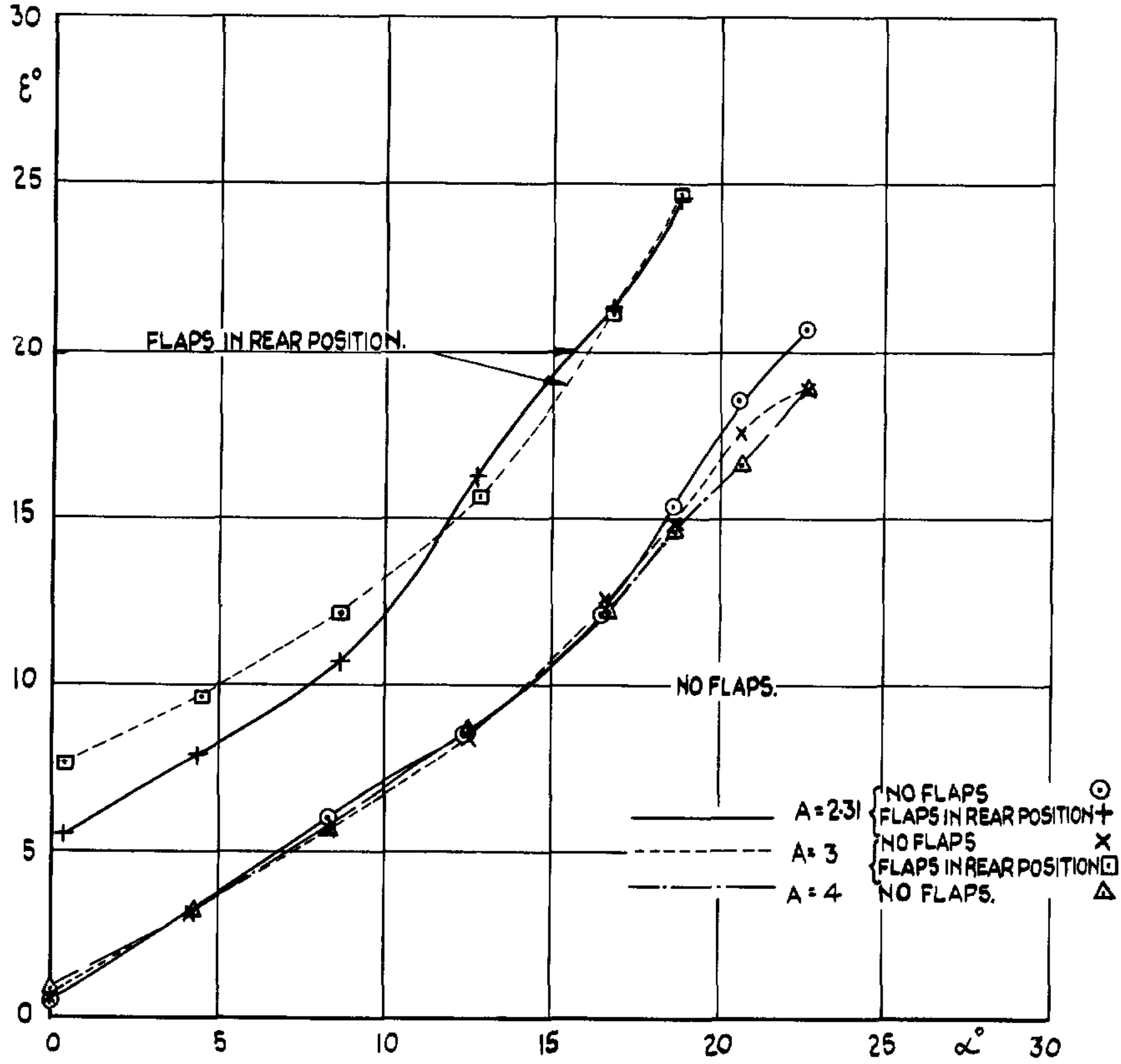

FIG. 8 DOWNWASH BEHIND A DELTA WING WITH AND WITHOUT SPLIT FLAPS. TAIL IN REAR POSITION AT MIDDLE HEIGHT.

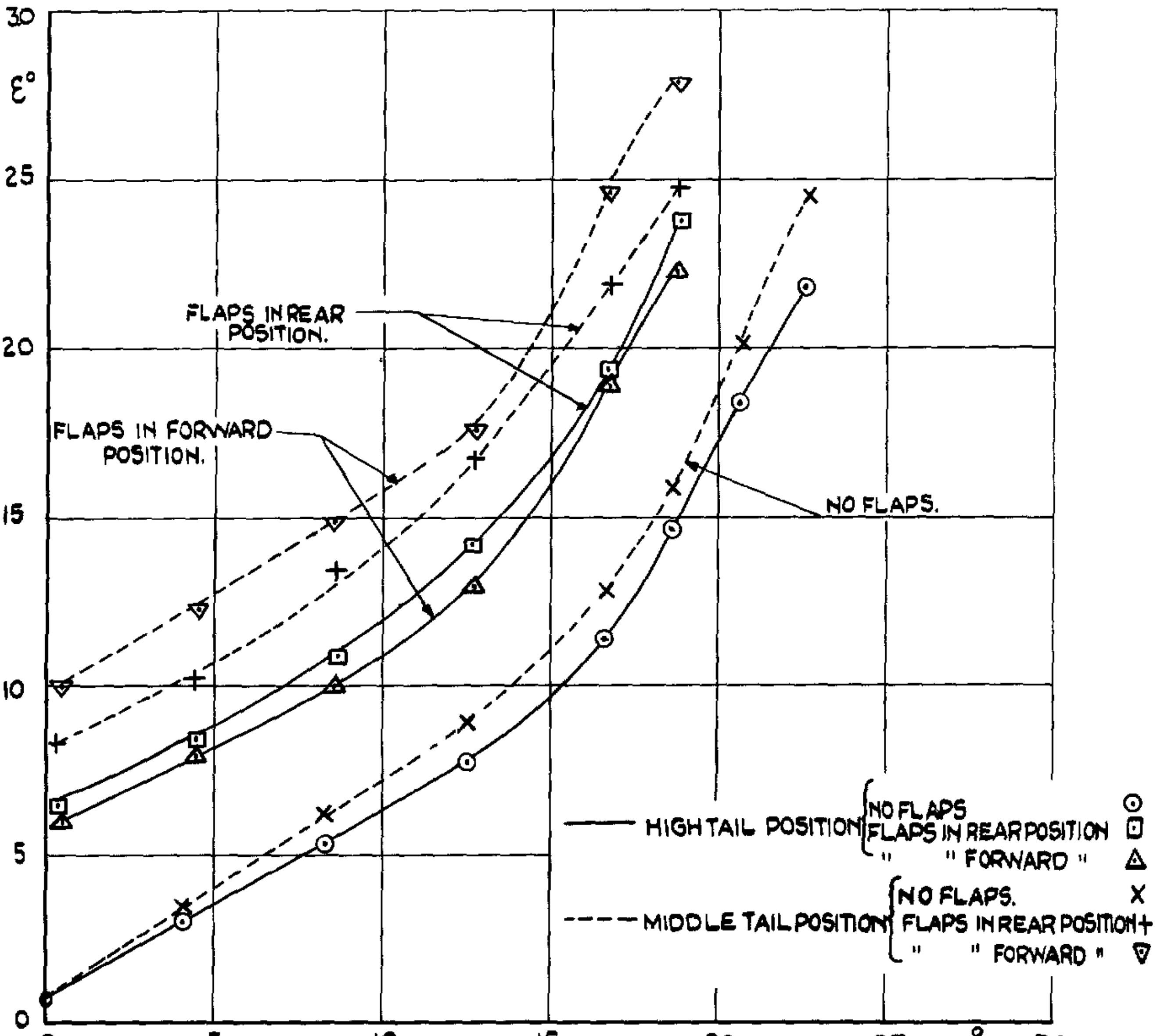

FIG. 9 DOWNWASH BEHIND A DELTA WING WITH AND WITHOUT SPLIT FLAPS. TAIL IN FORWARD POSITION $A = 3$.

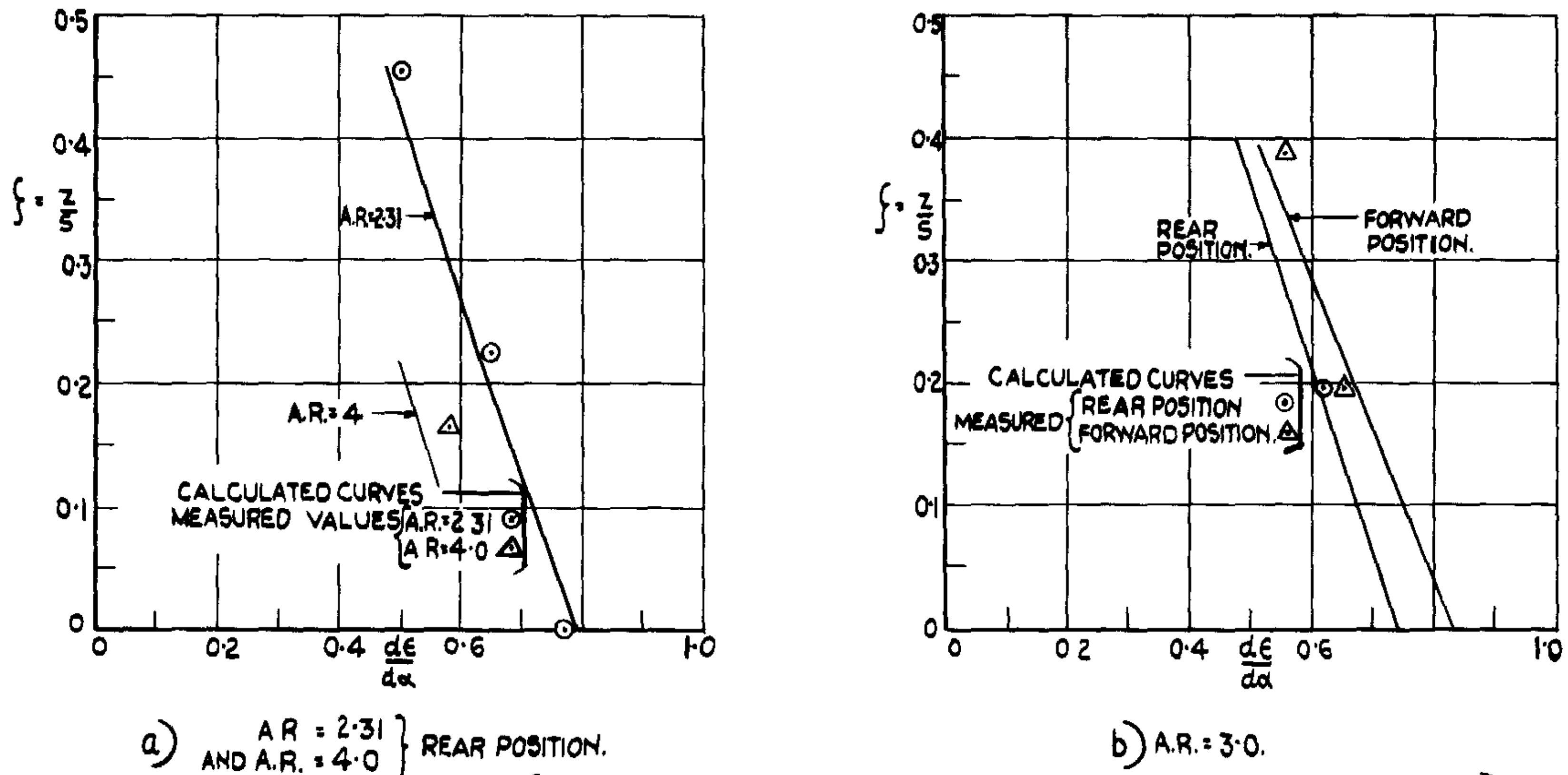

(THE EXPERIMENTAL VALUES OF $\frac{dC_L}{d\alpha}$ WERE USED FOR ALL CALCULATIONS.)

FIG.10(a&b). THEORETICAL AND EXPERIMENTAL VALUES OF $\frac{d\epsilon}{d\alpha}$ AT LOW INCIDENCES. NO FLAPS.

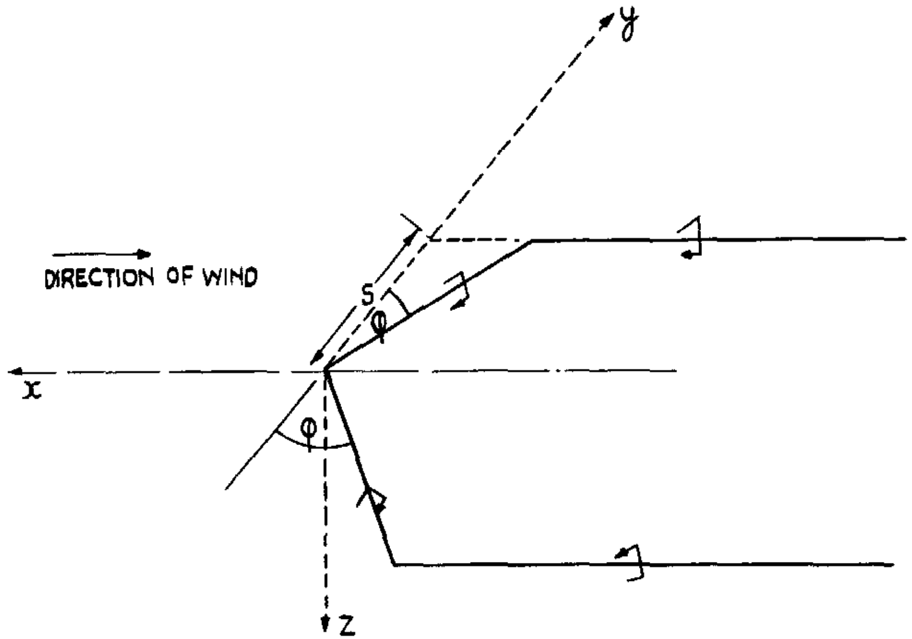

FIG.11(a) KINKED HORSHOE VORTEX SHOWING SYSTEM OF AXES.

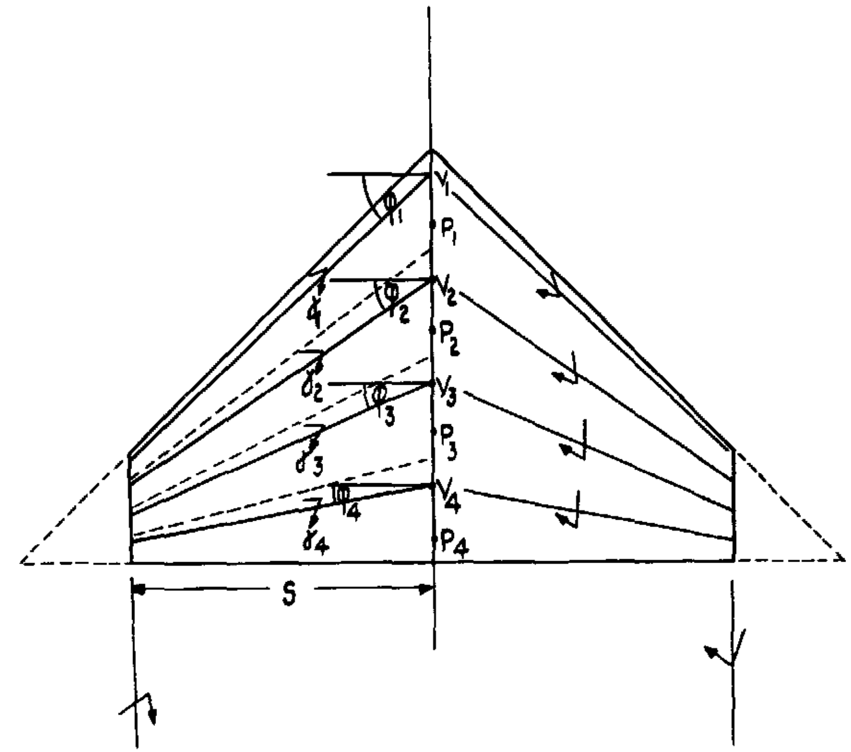

FIG 11(b) SYSTEM OF VORTICES USED FOR CALCULATIONS OF LIFT AND DOWNWASH ON A DELTA WING.

FIG.11(a&b)

C.P. No. 83
12,666, 12,000
A.R.C. Technical Report

PUBLISHED BY HER MAJESTY'S STATIONERY OFFICE

To be purchased from

York House, Kingsway, LONDON, W.C.2 : 429 Oxford Street, LONDON, W.1

P.O. Box 569, LONDON, S.E.1

13a Castle Street, EDINBURGH, 2 | 1 St. Andrew's Crescent, CARDIFF

39 King Street, MANCHESTER, 2 | Tower Lane, BRISTOL, 1

2 Edmund Street, BIRMINGHAM, 3 | 80 Chichester Street, BELFAST

or from any Bookseller

PRINTED IN GREAT BRITAIN

1952

Price 11s. 0d. net

S.O. Code No. 23-9006-83